

**Investigation of Cs<sub>2</sub>AgInBr<sub>6</sub> and Cs<sub>2</sub>AgGaBr<sub>6</sub> -based Double Perovskite Solar Cells: A Study of Solar Cell Parameters Using SCAPS-1D Simulation Software**

A DISSERTATION PROJECT REPORT  
SUBMITTED IN PARTIAL FULFILLMENT OF THE REQUIREMENTS  
FOR THE AWARD OF THE DEGREE  
OF  
MASTER OF SCIENCE  
IN  
**PHYSICS**

Submitted by: -

**SHUBHDA KAUSHIK (2K21/MSCPHY/46)**

**VISHAL DESWAL (2K21/MSCPHY/52)**

*under the guidance of*

**Dr. SARITA BAGHEL**

Assistant Professor

Department of Applied Physics



DEPARTMENT OF APPLIED PHYSICS  
DELHI TECHNOLOGICAL UNIVERSITY  
(Formerly Delhi College of Engineering)  
Bawana Road, Delhi-110042

## DECLARATION

We, SHUBHDA, (2K21/MSCPHY/46) and VISHAL DESWAL, (2K21/MSCPHY/52) hereby certify that the work which is presented in the Dissertation Project-II/Research work entitled “**Investigation of Cs<sub>2</sub>AgInBr<sub>6</sub> and Cs<sub>2</sub>AgGaBr<sub>6</sub> based Double Perovskite Solar Cells: A Study of Solar Cell Parameters Using SCAPS-1D Simulation Software**” in fulfilment of the requirement for the award of the degree of Master of Science in Physics and submitted to the Department of Applied Physics, Delhi Technological University, Delhi is an authentic record of our own, carried out during a period from August 2022 to May 2023, under the supervision of Dr SARITA BAGHEL. The matter presented in this report/thesis has not been submitted by me for the award of any other degree or any other Institute/University. The work on Cs<sub>2</sub>AgGaBr<sub>6</sub> based double perovskite solar cell has been communicated in peer reviewed Scopus indexed conference and another work on Cs<sub>2</sub>AgInBr<sub>6</sub> based double perovskite solar cell has been communicated in SCOPUS and SCI indexed journal, with the following details:

1. <b>Title of the Paper</b>	To study the impact of several ETLs and HTLs on the Cs <sub>2</sub> AgGaBr <sub>6</sub> based double perovskite solar cell using SCAPS-1D
<b>Author names</b>	Shubhda Kaushik, Vishal Deswal Rahul kundara, Sarita Baghel
<b>Name of Conference</b>	International Conference on Advanced Materials for Emerging Technologies (ICAMET-2023)
<b>Status of Paper</b>	Communicated
<b>Date and venue of conference</b>	May 04-06, 2023; Netaji Subhas University of Technology, New Delhi– 110078 (India)
<b>Conference registered</b>	yes
<b>Date of publication</b>	Yet to be published

2. <b>Title of the Paper</b>	Numerical simulation of highly efficient Cs <sub>2</sub> AgInBr <sub>6</sub> -based Double Perovskite Solar Cell using SCAPS 1-D
<b>Author names</b>	Vishal Deswal, Shubhda Kaushik, Rahul kundara, Sarita Baghel
<b>Name of journal</b>	Materials Science and Engineering B (MSEB)
<b>Status of Paper</b>	Communicated
<b>Date of communication</b>	12 <sup>th</sup> may 2023
<b>Date of acceptance</b>	
<b>Date of publication</b>	

Place: Delhi

SHUBHDA (2K21/MSCPHY/46)

Date:

VISHAL DESWAL (2K21/MSCPHY/52)

### SUPERVISOR CERTIFICATE

To the best of my knowledge, the above work has not been submitted in part or full for any Degree or Diploma to this University or elsewhere. I, further certify that the publication and indexing information given by the students is correct.

Place: Delhi

Dr. Sarita Baghel

Date:

SUPERVISOR

## ABSTRACT

In Perovskite to get rid of toxicity of lead-based perovskite solar cell and to increase its efficiency various Materials are under research among them double perovskite solar cells (DPSCs) are promising with high efficiency. Lead free DPSCs recently attracted lots of research Interest because of its viability as a promising perovskite absorber layer in the device architecture along with its reasonable cost, remarkable stability and high performance. The lead and non-biodegradable material-based Perovskite solar cells (PSCs) are still a hurdle to its commercialization.

Cs<sub>2</sub>AgGaBr<sub>6</sub>-based DPSC promised high efficiency in previous studies and we investigate it further. ZnSe, IGZO, WS<sub>2</sub>, TiO<sub>2</sub>, ZnO and CeO<sub>2</sub> were chosen as ETLs, while Spiro-OMeTAD, CuO, PEDOT: PSS, P3HT, CBTS, and Cu<sub>2</sub>O were chosen as HTLs. Using the SCAPS-1D solar cell simulation program, we thoroughly investigated the properties of solar cell layers to determine the optimum structure: CBTS/Cs<sub>2</sub>AgGaBr<sub>6</sub>/ZnSe. ETL and HTL with high mobility of charge carriers and absorption coefficient is required for desired performance of DPSC. Cs<sub>2</sub>AgGaBr<sub>6</sub> exhibits a direct bandgap of 1.42 eV and a semiconducting nature. In order to attain the highest possible power conversion efficiency (PCE), the device structure of multiple cells was examined. Of these, a cell with ZnSe based ETL and CBTS based HTL produced best efficiency, 30.26% at a thickness of 600 nm.

We have also investigated a non-toxic inorganic material i.e., Cs<sub>2</sub>AgInBr<sub>6</sub> using SCAPS-1D software. we optimized various parameters like Defect density ( $N_t$ ), thickness, operating temperature and electron affinity ( $\chi$ ) of perovskite absorber layer (Cs<sub>2</sub>AgInBr<sub>6</sub>). Effect of various ETLs and HTLs on the performance device is also analyzed. At absorber layer thickness of 600 nm, the Cs<sub>2</sub>AgInBr<sub>6</sub>-based DPSC has achieved maximum efficiency of 26.9%. The optimized value of  $N_t$  is  $10^{14}$  and operating temperature is 300 K

**DELHI TECHNOLOGICAL UNIVERSITY**

(Formerly Delhi College of Engineering)

Bawana Road, Delhi - 110042

**ACKNOWLEDGEMENT**

We would like to express our deepest gratitude to Dr. Sarita Baghel, whose guidance and support were invaluable throughout the completion of our M.Sc. dissertation. Her profound knowledge, insightful suggestions, and constant encouragement have been instrumental in shaping our research work and enhancing its quality. Dr. Baghel's dedication and commitment to her students' academic growth have been truly inspiring, and we are grateful for the opportunity to learn under her guidance.

We would also like to extend our sincere appreciation to the Department of Applied Physics at Delhi Technological University for providing the necessary resources and infrastructure that facilitated the smooth execution of our research work. The department's commitment to fostering a conducive academic environment and its emphasis on practical learning have been pivotal in our development as researchers.

Furthermore, we are indebted to the faculty members and staff of the Department of Applied Physics for their valuable insights and assistance during the course of our studies. Their expertise and willingness to share knowledge have greatly contributed to our understanding of the subject matter.

We would also like to express our gratitude to our fellow classmates and colleagues for their constant support and collaboration. Our discussions and interactions have been instrumental in shaping our research ideas and broadening our perspective.

In conclusion, we extend our heartfelt appreciation to Dr. Sarita Baghel and the Department of Applied Physics at Delhi Technological University for their invaluable guidance, support, and resources. Their contributions have played a crucial role in the successful completion of our M.Sc. dissertation and our overall academic growth.

**SHUBHDA**

**VISHAL DESWAL**

## Table of Contents

<b>DECLARATION .....</b>	<b>ii</b>
<b>SUPERVISOR CERTIFICATE.....</b>	<b>iii</b>
<b>ABSTRACT.....</b>	<b>iv</b>
<b>ACKNOWLEDGEMENT .....</b>	<b>v</b>
<b>Table of Contents .....</b>	<b>vi</b>
<b>LIST OF TABLES.....</b>	<b>viii</b>
<b>LIST OF FIGURES.....</b>	<b>ix</b>
<b>Chapter1 Introduction.....</b>	<b>1</b>
1.1 Background .....	1
1.2 Research Objectives .....	2
1.3 Significance of the Research: .....	2
1.3.1 Advancement of PSC Technology .....	3
1.3.2 Enhanced Efficiency and Stability.....	3
1.3.3 Novel Material Exploration: .....	3
1.3.4 Sustainable Energy Solutions .....	3
<b>Chapter2 Literature Review .....</b>	<b>4</b>
2.1 Perovskite Solar Cells .....	4
2.2 Double Perovskite Solar Cells.....	5
2.3 $\text{Cs}_2\text{AgInBr}_6$ .....	5
2.4 $\text{Cs}_2\text{AgGaBr}_6$ .....	6
2.5 SCAPS-1D Solar Cell Simulation Software .....	8
2.5.1 Working Principle .....	8
2.5.2 Uses of SCAPS-1D .....	9
2.5.3 Underlying Codes and Concepts .....	9
2.5.4 Numerical method used in SCAPS-1D .....	10
<b>Chapter3 Methodology .....</b>	<b>12</b>

3.1 Cs <sub>2</sub> AgGaBr <sub>6</sub> .....	12
3.1.1 Device Structure .....	12
3.1.2 Procedure .....	12
3.2 Cs <sub>2</sub> AgGaBr <sub>6</sub> .....	15
3.2.1 Structure.....	15
3.2.2 DPSC design methodology .....	16
<b>Chapter4 Results and Discussion .....</b>	<b>20</b>
4.1 Cs <sub>2</sub> AgGaBr <sub>6</sub> .....	20
4.1.1 Study of different ETL layers.....	21
4.1.2 Study of HTL layers .....	21
4.2 Cs <sub>2</sub> AgInBr <sub>6</sub> .....	24
4.2.1 Variation of HTLs and ETLs .....	24
4.2.2 Optimization of Absorber layer Defect density (N <sub>t</sub> ) .....	27
4.2.3 Optimization of thickness of absorber layer .....	29
4.2.4 Effect of Temperature.....	30
4.2.5 Optimization of Electron affinity .....	31
4.3 CBTS HTL.....	32
4.4 HTL has larger impact than ETL on solar cell.....	33
<b>Chapter5 Conclusion .....</b>	<b>35</b>
5.1 Cs <sub>2</sub> AgGaBr <sub>6</sub> .....	35
5.2 Cs <sub>2</sub> AgInBr <sub>6</sub> .....	35
<b>APPENDICES .....</b>	<b>36</b>
<b>References.....</b>	<b>43</b>

Appendix 1	Plagiarism report
Appendix 2	Abstract acceptance mail (Paper 1)
Appendix 3	Registration slip for proof of conference registration
Appendix 4	Certificate of conference
Appendix 5	Proof of SCOPUS indexing
Appendix 6	Submission mail (Paper 2)
Appendix 7	Proof of SCOPUS indexing of journal

### LIST OF TABLES

TABLE NUMBER	CAPTION	PAGE NUMBER
Table 3.1	Various ETL parameters	13
Table 3.2	Various HTL parameters	14
Table 3.3	Table for Parameters of (a) CBTS (b)perovskite layer (Cs <sub>2</sub> AgGaBr <sub>6</sub> ) (c) ZnSe (d) FTO	15
Table 3.4	Simulation parameters of initial DPSC layers.	17
Table 3.5	Simulation parameters of various HTL	18
Table 3.6	Simulation parameters of various ETLs	19
Table 4.1	Different cell structures and their simulation results	22
Table 4.2	Different cell structure and their simulation results	27



## LIST OF FIGURES

FIGURE NUMBER	CAPTION	PAGE NUMBER
Figure 3.1	Device Structure for simulation and band alignment diagram	12
Figure 3.2	Device structure and band gap alignment for Cs <sub>2</sub> AgInBr <sub>6</sub> based DPSC	16
Figure 4.1	Graphs of (a)QE vs wavelength for various ETL layers (b) J-V curve for various ETL layers	21
Figure 4.2	Graphs of (a)QE vs wavelength for various HTL layers (b) J-V curve for various HTL layers	22
Figure 4.3	Graphs of (a)QE vs wavelength for optimized cell (b) J-V curve for optimized cell structure	24
Figure 4.4	Graphs of (a) J <sub>sc</sub> VS Voltage (b) QE vs wavelength with ZnSe as ETL and varying HTLs	25
Figure 4.5	Graphs of (a) J <sub>sc</sub> VS Voltage (b) QE vs wavelength with TiO <sub>2</sub> as ETL and varying HTLs	26
Figure 4.6	Graphs of (a) J <sub>sc</sub> VS Voltage (b) QE vs wavelength with IGZO as ETL and varying HTLs	26
Figure 4.7	Graph showing change in various DPSC parameters as a function of defect density, N <sub>t</sub>	28
Figure 4.8	Graph showing change in various DPSC parameters as a function of thickness	29
Figure 4.9	Graph showing change in various DPSC parameters as a function of Temperature	30
Figure 4.10	Graph showing change various DPSC parameters as a function of electron affinity	32

## LIST OF ABBREVIATIONS

Symbol/index	Meaning/Abbreviation
PCE	Power Conversion Efficiency
ZnSe	Zinc Selenide
CBTS	Copper Barium Thiostannate
FF	Fill Factor
ETL	Electron Transport Layer
HTL	Hole Transport Layer
FTO	Flourine Tin Oxide
Cs <sub>2</sub> AgGaBr <sub>6</sub>	Cesium Silver Gallium Bromide
Cs <sub>2</sub> AgInBr <sub>6</sub>	Cesium Silver Indium Bromide
TMM	Transfer Matrix Mode
DPSC	Double Perovskite Solar Cell
QE	Quantum Efficiency
E <sub>g</sub>	Band Gap
$\chi$	Electron Affinity
N <sub>t</sub>	Defect Density
$\mu_e$	Electron Mobility
$\mu_h$	Hole mobility
N <sub>c</sub>	Conduction band effective density of states
N <sub>v</sub>	Valence band effective density of states
$\epsilon_r$	Dielectric Permittivity
J <sub>sc</sub>	Current density
V <sub>oc</sub>	Voltage
DHP	Double Halide Perovskites
K	Kelvin
V <sub>e</sub>	Electron Thermal velocity
V <sub>h</sub>	Hole Thermal velocity

## Chapter1 Introduction

### 1.1 Background

A safe and inexhaustible renewable energy source is solar power, that holds great potential for addressing global energy demands and reducing carbon emissions. Significant research efforts have been made over the years to create more efficient, economical, and stable solar cell. The conventional silicon and other inorganic semiconductor-based photovoltaics dominated market as they offer established performance and reliability. However, their high production costs and limited flexibility have sparked interest in exploring alternatives. PSCs are emerging as strong candidates for upcoming advanced and efficient photovoltaics.

PSCs are based on organic-inorganic metallic halide perovskite materials. These materials are typically denoted by  $ABX_3$  (A and B are organic and metal cations respectively; x= halide anion). Characteristics like tuneable bandgap and high absorption coefficient enable PSCs to achieve high PCE and low-cost fabrication processes, making them a potentially disruptive technology in the solar cell industry.

Despite their impressive performance, traditional PSCs face challenges regarding stability, material toxicity, as well as moisture sensitivity. In recent years, researchers have turned their attention to double perovskite materials as an alternative approach for better stability and performance of PSCs

Double perovskite materials, also known as mixed-halide or mixed-cation perovskites, are composed of two different metal cations in the B-site of the perovskite structure. This modification introduces enhanced freedom in controlling the material properties, including stability, bandgap, and defect tolerance. By carefully engineering the composition of the double perovskite materials, it is possible to tailor their optoelectronic properties to meet the requirements of efficient solar cell operation.

Due of their possible advantages, such as improved stability, reduced toxicity, and enhanced light harvesting capabilities. research into DPSCs has received a lot of interest. Researchers have reported encouraging results in terms of efficiency, long-term stability, and resistance to moisture and heat. However, the understanding of

double perovskite materials and their performance in solar cells is still in its early stages, necessitating further investigation and optimization.

In this context, this study's goal is to look into the capabilities and characteristics of DPSCs. The research will involve synthesizing and characterizing different double perovskite compositions, fabricating solar cell devices, and evaluating their optoelectronic properties, stability, and device performance. This study opens way for further research on double perovskite materials and pave the way for their potential implementation in efficient and stable solar cell technologies.

By addressing the limitations of traditional PSCs, DPSCs offer an exciting avenue for advancing the field of photovoltaics and driving the development of sustainable energy solutions.

## 1.2 **Research Objectives:**

Primary aim of this study on  $\text{Cs}_2\text{AgInBr}_6$  and  $\text{Cs}_2\text{AgGaBr}_6$  based double perovskite solar cells are as follows:

- 1.2.1 **Device Fabrication:** The next objective is to fabricate solar cell devices using the double perovskite materials as the active layer. The devices will be constructed using suitable device architectures in SCAPS-1D. Optimization of the device fabrication parameters will be carried out to enhance the device performance.
- 1.2.2 **Performance Evaluation:** one of the primary goals is to evaluate the optoelectronic properties and performance of the  $\text{Cs}_2\text{AgInBr}_6$  and  $\text{Cs}_2\text{AgGaBr}_6$  based double perovskite solar cells. This includes measuring key parameters like PCE, J-V characteristics, Fill factor and Q.E.
- 1.2.3 **Analysis and Optimization:** The final objective is to analyze the obtained results and identify strategies to optimize the performance of  $\text{Cs}_2\text{AgInBr}_6$  and  $\text{Cs}_2\text{AgGaBr}_6$  DPSCs. The objective remains to improve DPSCs PCE and performance.

## 1.3 **Significance of this Research:**

This research on  $\text{Cs}_2\text{AgInBr}_6$  and  $\text{Cs}_2\text{AgGaBr}_6$  based double perovskite solar cells holds significant importance for several reasons:

- 1.3.1 **Advancement of PSC Technology:** By investigating the performance of  $\text{Cs}_2\text{AgInBr}_6$  and  $\text{Cs}_2\text{AgGaBr}_6$  double perovskite materials in solar cells, this research contributes to significant progress of PSC technology. It expands the knowledge base and understanding of the unique properties and potential advantages of double perovskites as active materials.
- 1.3.2 **Enhanced Efficiency and Stability:** Double perovskite materials offer the potential for improved efficiency and stability compared to traditional perovskite materials. By exploring  $\text{Cs}_2\text{AgInBr}_6$  and  $\text{Cs}_2\text{AgGaBr}_6$  double perovskites, this research aims to uncover the performance benefits that these materials can bring to solar cell devices, such as enhanced charge transport, reduced defects, and improved stability under operating conditions.
- 1.3.3 **Novel Material Exploration:** The study of  $\text{Cs}_2\text{AgInBr}_6$  and  $\text{Cs}_2\text{AgGaBr}_6$  double perovskites expands the range of materials available for solar cell applications. These materials offer different compositional and structural properties compared to conventional perovskites, opening up new possibilities for tailoring the optoelectronic properties of solar cells.
- 1.3.4 **Sustainable Energy Solutions:** Developing efficient as well as stable photovoltaics is crucial for advancing sustainable energy solutions. By improving the understanding and performance of  $\text{Cs}_2\text{AgInBr}_6$  and  $\text{Cs}_2\text{AgGaBr}_6$  DPSCs, this research helps in achieving the broader goal of realizing cost-effective and environmentally friendly photovoltaic devices.

## **Chapter2**

## Chapter2 Literature Review

### 2.1 Perovskite Solar Cells

Undoubtedly, we have a significant requirement for electricity because of the world's population growth. In past years, fossil fuels have been main source of electricity, but as conventional energy sources become scarcer, people are increasingly turning to pure, non-polluting energy sources. Both directly and tangentially using solar energy as a source of heat is possible. Therefore, extensive research is required to create such devices that can effectively recapture the massive thermal energy produced as waste in various energy as well as available naturally through sun. For the sake of human sustainability in this respect, research into novel renewable energy sources is essential. In this view, photons to energy conversion are a preferred approach for advancement of civilization. Perovskite solar cells among other such devices attract attention of researchers because of a number of distinctive features like cost efficacy, simple manufacturing, outstanding efficiency etc.

Because of their exceptional physical and/or chemical characteristics, such as their structure, optical properties, electrical properties, superconducting, catalytic, and magnetic properties perovskite materials have recently helped a number of technologies[1]–[3]. More precisely, organic-inorganic perovskites  $ABX_3$  with halogens (Cl, Br, I) as anions at X-site and lead as a cation at B-site have revolutionized the field of photovoltaic study[4], [5].

Devices manufactured based on halide perovskites demonstrated a significant improvement in efficiency (3.8% to 25.5%) which is better than silicon thin-film solar cells. lead-based perovskites subjected to air, heat, or moisture shows degrading tendency; as a result, manufacturing of the solar cells require more sophisticated enclosure methods than silicon[6]. In addition, due to the high lead concentration in these compounds, the environmental effect is a worry in light of the anticipated widespread use of perovskite-based solar cells [7], [8]. Meanwhile, Pb-free perovskite compounds with exceptional ecological resilience have become an emerging study challenge in light of such environmental concerns[9], [10].

Many significant attempts have been made over the past decade in order to reduce the danger of Pb present in perovskites, particularly by enhancing their dimension and/or makeup. A  $M^+$  monovalent and a  $M'^{3+}$  trivalent cations are previously shown as substitute the  $2Pb^{2+}$  creating 3-D “Double-halide perovskites” (DHPs) having formula  $A_2MM'X_6$ . here, A can be Cs, Rb, K, Na; and M can be Cu, Ag, Au, In;  $M' = Bi, Sb, In, Ga$ ;  $X = I, Br, Cl$ .[11], [12]. Research shows that in thermoelectric, optoelectronic, and/or photovoltaic applications, gallium and silver atoms based non-toxic perovskite materials are superior to perovskites based on lead. [13]

## 2.2 Double Perovskite Solar Cells

High-performance PSCs are unstable. Additionally, they are based on toxic lead [[14]. Unquestionably, this severely restricts their usage in solar systems. As an alternative, a new generation of DPSC material has been proposed to address the issue [15]–[17]. The suggested compounds have been successfully synthesized and are inorganic, stable, and non-toxic[15]–[19]. These are therefore excellent choices for photovoltaic applications.

## 2.3 Cs<sub>2</sub>AgInBr<sub>6</sub>

Cs<sub>2</sub>AgInBr<sub>6</sub> is a double perovskite material which garnered significant attention as it offers useful characteristics and possible applications in solar cells. This material belongs to halide double perovskites and has a crystal structure composed of cesium (Cs), silver (Ag), indium (In), and bromine (Br) atoms.

Cs<sub>2</sub>AgInBr<sub>6</sub> is one of the double perovskites materials that has been touted as a top contender for technological applications, particularly in the solar industry hence receiving a lot of attention recently. Only a few data were given about the material's optical and electrical characteristics, which are crucial for the design and fabrication of devices that utilize the perovskite in question[20], [21], despite several fundamental aspects of the material being researched[22]–[24].

The Cs<sub>2</sub>AgInBr<sub>6</sub> double perovskite exhibits several desirable properties which makes it attractive for solar cell applications:

1. **Optoelectronic Properties:** Cs<sub>2</sub>AgInBr<sub>6</sub> possesses a direct bandgap in the visible light range, enabling efficient absorption of sunlight. This property is crucial for photovoltaics because it allows for effective conversion of solar energy into electrical energy.
2. **High Absorption Coefficient:** The material in question has a high absorption coefficient, which enables it to absorb a large number of photons even when the film thickness is relatively thin. This property is advantageous for fabricating thin-film solar cells, reducing material usage and cost.
3. **Long Carrier Diffusion Length:** Cs<sub>2</sub>AgInBr<sub>6</sub> possess a long carrier diffusion length, indicating that the photogenerated charges can go far into the material without recombining. within material with no recombination. This characteristic is essential for charge extraction and collection, leading to higher solar cell efficiencies.

4. **Thermal Stability:** Because of its great thermal stability,  $\text{Cs}_2\text{AgInBr}_6$  can survive high temperatures without suffering considerable deterioration. For the manufacture and long-term reliability of solar cells, particularly under actual working circumstances, this characteristic is crucial.

5. **Low Toxicity:** Compared to some other halide perovskites,  $\text{Cs}_2\text{AgInBr}_6$  has relatively low toxicity, which is advantageous for large-scale manufacturing and potential commercialization of photovoltaics.

The unique combination of these properties makes  $\text{Cs}_2\text{AgInBr}_6$  an intriguing candidate for solar cell applications. Researchers are actively exploring its potential to develop highly efficient and DPSC. Some of the key areas of research and development include:

1. **Device Optimization:** Researchers are working for improving the PCE of  $\text{Cs}_2\text{AgInBr}_6$ -based DPSCs by optimizing device architectures, interface engineering, and charge transport properties.

2. **Stability Enhancement:** Ensuring enduring stability of  $\text{Cs}_2\text{AgInBr}_6$ -based DPSC is a crucial area of focus. Researchers are investigating strategies to enhance the material's resistance to moisture, heat, and light-induced degradation, thereby improving the operational lifetime of the solar cells.

3. **Scale-Up and Manufacturing:** Efforts are underway to develop scalable fabrication techniques for  $\text{Cs}_2\text{AgInBr}_6$  solar cells, enabling their large-scale production at low cost. This includes exploring solution-based deposition methods, roll-to-roll processing, and compatibility with existing manufacturing infrastructure.

The application of  $\text{Cs}_2\text{AgInBr}_6$  in solar cells holds promise for realizing high-efficiency, cost-effective, and environmentally friendly photovoltaic devices. Ongoing studies aim to overcome these challenges associated with stability, efficiency, and scalability, therefore making way for commercialization of  $\text{Cs}_2\text{AgInBr}_6$ -based solar cells and contributing to the clean energy transition.

#### **2.4 $\text{Cs}_2\text{AgGaBr}_6$**

Research shows that in thermoelectric, optoelectronic, and/or photovoltaic applications, gallium and silver atoms based non-toxic perovskite materials are superior to perovskites based on lead. [13]

In the absence of interface imperfections,  $\text{Cs}_2\text{AgGaBr}_6$ 's favorable bandgap of 1.42 eV along with strong absorption leads to a high PCE of 34.99%. this corresponds to



ideal thickness of 2.6 micro-m. Yet, the efficiency is reduced to 30.90% by adding interface defects[13]. In light of this we therefore attempt to study the effect of different HTL/ETL layers to study and compare their effect on efficiency of solar cell, at a lower thickness than the optimum of 2.6micrometer.[13] (As this is considered much thicker); instead, we used standard 600nm as thickness.

$\text{Cs}_2\text{AgGaBr}_6$  (also referred to as Cesium Silver Gallium Bromide) is indeed a double perovskite material that has gained attention for its potential application in solar cells. This material consists of cesium (Cs), silver (Ag), gallium (Ga), and bromine (Br) atoms in its crystal structure.

While specific information  $\text{Cs}_2\text{AgGaBr}_6$  may be limited due to its relatively recent discovery and ongoing research, we can discuss some general properties and potential applications of double perovskite materials in solar cells.

- 1) **Optoelectronic Properties:** Double perovskite materials like  $\text{Cs}_2\text{AgGaBr}_6$  typically possess desirable optoelectronic properties, including a suitable bandgap for solar absorption and efficient charge carrier transport. These properties are crucial for effective light absorption and energy conversion in solar cells.
- 2) **Tunability:** Double perovskite materials have several benefits, including the possibility of tuning their bandgap and electronic properties by altering their composition and structure. This tunability allows researchers to optimize the material for specific solar cell applications and tailor it to maximize device performance.
- 3) **High Absorption Coefficient:** Double perovskites often display a high absorption coefficient. This property makes efficient absorption of light possible even for thin films. This characteristic can facilitate the development of thin-film DPSCs, decreasing material usage and cost.
- 4) **Carrier Transport:** Highly efficient PSCs require effective carrier transport. Double perovskite materials can have favourable charge carrier mobilities, enabling the effective extraction and collection of photogenerated electrons and holes.
- 5) **Stability:** Ensuring the prolonged stability of PSCs is challenging. Ongoing research aims for improving stability of DPSC materials, including  $\text{Cs}_2\text{AgGaBr}_6$  by addressing issues such as moisture sensitivity, thermal stability, and resistance to degradation.

Regarding the specific application of  $\text{Cs}_2\text{AgGaBr}_6$  in DPSCs, it is important to notice that the material is relatively new, and research on its solar cell performance and

optimization is still in progress. Researchers are likely exploring the fabrication methods, device architectures, and stability considerations to determine the viability and potential advantages of  $\text{Cs}_2\text{AgGaBr}_6$ -based solar cells.

Overall, while specific information about  $\text{Cs}_2\text{AgGaBr}_6$  may be limited, double perovskite materials are desirable for solar cell applications due to their general characteristics. Ongoing research in PSCs aims to achieve stability, enhance efficiency, and improve the scalability of these materials for commercialization in the renewable energy sector.

## **2.5 SCAPS-1D Solar Cell Simulation Software**

This section provides an overview of SCAPS-1D, a popular program for simulating solar cells. It describes its capabilities in modeling and simulating various solar cell parameters, such as electrical and optical properties, carrier transport, and recombination mechanisms. The subsection also emphasizes the importance of simulation software in solar cell research, allowing researchers to optimize device performance and gain insights into the underlying physics.

SCAPS-1D is a simulation software tool specifically designed for modeling and simulating the performance of photovoltaics. It provides a platform for analyzing and optimizing the electronic and optical properties of various types of photovoltaics, including and not constrained to silicon-based, thin-film, and perovskite solar cells. Here's an overview of how SCAPS-1D works, its uses, underlying codes, and concepts:

### **2.5.1 Working Principle:**

SCAPS-1D utilizes a numerical approach to simulate the behavior of solar cells. It employs a one-dimensional modeling framework, considering the device structure in the form of layers along the thickness direction. By solving a set of coupled differential equations, SCAPS-1D calculates and predicts various parameters, such as J-V characteristics, Q.E., carrier density profiles, and electric fields within the solar cell structure.

### **2.5.2 Uses of SCAPS-1D:**

1. **Device Design and Optimization:** SCAPS-1D enables researchers and engineers to explore different device architectures, layer materials, and parameters to optimize solar cell performance. It aids in the design process by predicting the effects of various changes on the electrical output, helping identify strategies to enhance efficiency.
2. **Parameter Extraction:** The software allows users to extract and determine important material and device parameters, such as carrier lifetimes, interface recombination velocities, trap densities, and mobility values. These extracted parameters can give insightful information on material's quality and interfaces within the solar cell structure.
3. **Sensitivity Analysis:** SCAPS-1D facilitates sensitivity analysis, allowing users to evaluate the impact of variations in material properties, layer thicknesses, and other parameters on the device performance. This analysis aids in identifying critical parameters that significantly influence solar cell efficiency and guides experimental efforts.

### **2.5.3 Underlying Codes and Concepts:**

SCAPS-1D is built on a foundation of physical models and mathematical equations that describe the behavior of solar cells. The software employs numerical methods and iterative algorithms to solve these equations and simulate the device operation. Some of the underlying concepts and codes used in SCAPS-1D include:

1. **Drift-Diffusion Equations:** SCAPS-1D employs the drift-diffusion model, which incorporates charge carrier transport mechanisms like diffusion brought on by gradients in carrier concentration and drift brought on by electric fields. These equations describe the movement of electrons and holes within the solar cell structure.
2. **Shockley-Read-Hall (SRH) Recombination:** The SRH model accounts for the recombination of charge carriers at defect sites within the material. SCAPS-1D includes algorithms to calculate and incorporate the impact of SRH recombination on device performance.
3. **Optical Modelling:** SCAPS-1D considers the absorption and transmission of light within the solar cell structure. It utilizes concepts like Lambert-Beer's law to

account for light absorption in different layers and interfaces, considering the wavelength-dependent optical properties of materials.

4. **Interface and Contact Models:** The software includes models to characterize the electrical behaviour and recombination properties at material interfaces and contacts, accounting for phenomena such as surface recombination and tunnelling.

5. **Parameter Fitting:** SCAPS-1D incorporates fitting routines and optimization algorithms to comparison between simulation and experimental results. This allows for determination of accurate material and device parameters that best replicate the measured device characteristics.

Overall, SCAPS-1D leverages a combination of physics-based models, numerical methods, and optimization algorithms to simulate and analyze the performance of photovoltaics. By providing a comprehensive platform for device design, optimization, and parameter extraction, SCAPS-1D contributes to the advancement of solar cell technology and enables researchers and engineers to explore new avenues for enhancing solar energy conversion efficiency.

#### **2.5.4 Numerical method used in SCAPS-1D: -**

SCAPS-1D utilizes a numerical method called the Transfer Matrix Method (TMM) for solving the electrical and optical equations for the simulation of photovoltaic devices. The TMM is a powerful technique for modeling multi-layered structures by considering the transmission and reflection of light at each interface within the structure. The TMM implemented in SCAPS-1D allows for the calculation of optical properties, such as absorption and transmission coefficients, as well as the propagation of light through the various layers of the solar cell. This information is crucial for accurately modeling the absorption of photons and calculating the Q.E. of the device.

In addition to the TMM, SCAPS-1D incorporates other numerical methods to solve the drift-diffusion equations that describe the carrier transport and recombination within the solar cell structure. These methods typically involve the discretization of the device structure into a set of computational points or nodes along the thickness direction, and the solution of the resulting set of coupled differential equations. While the exact details of the specific code implementation in SCAPS-1D are not

publicly disclosed, it likely employs well-established numerical algorithms, such as finite difference or finite element methods, to solve the drift-diffusion equations. These methods approximate the derivatives in the equations using discrete differences and iteratively solve the resulting equations to obtain the carrier profiles and device characteristics.

It's important to note that SCAPS-1D is a proprietary software tool, and the specific implementation details, including the choice of algorithms and coding techniques, are not publicly available. The underlying numerical methods and codes used in SCAPS-1D are likely optimized for efficiency and accuracy in simulating solar cell devices, providing researchers and engineers with a reliable platform for their investigations and optimizations.

## Chapter3 Methodology

### 3.1 Cs<sub>2</sub>AgGaBr<sub>6</sub>

#### 3.1.1 Device Structure

(FTO/ETL/Cs<sub>2</sub>AgGaBr<sub>6</sub>/HTL/Au) device structure is used for the study of Cs<sub>2</sub>AgGaBr<sub>6</sub> based DPSC. This is also shown in Figure 3.1. During all the simulations only parameters of ETL and HTL changes according to layers used. The parameters of FTO and perovskite layers are same for all simulations and are mentioned in Table 3.3. The back contact used in simulation is that of Au and is same for all simulations.

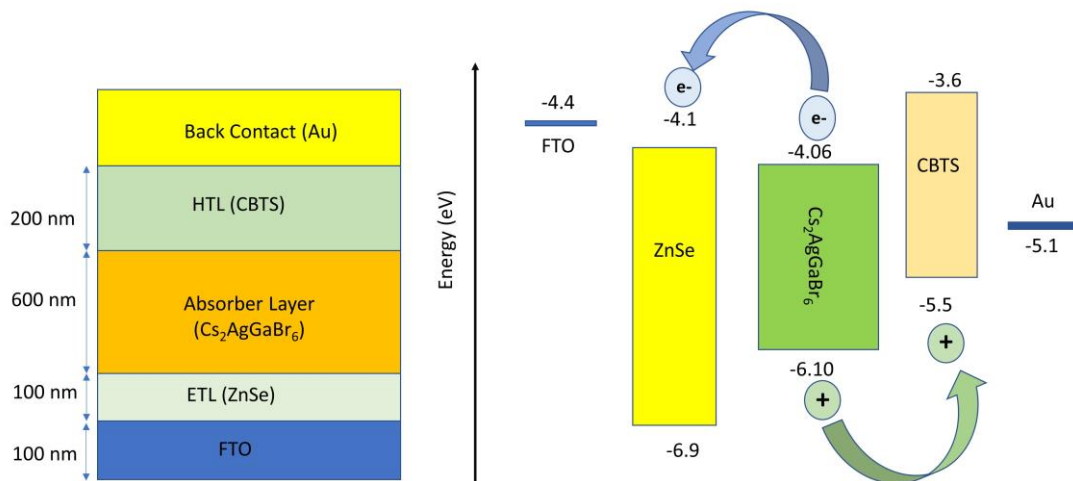


Figure 3.1:- Device Structure for simulation and band alignment diagram

#### 3.1.2 Procedure

The device was fabricated as shown in the Table 3.1; with a transparent ETL, following which there is perovskite photon absorbing layer and holes transport layer forming (n-i-p) type structure. This fabrication in SCAPS can be achieved by navigating through set problem option and adding respective layers. The different

layers and their parameters are mentioned in the Table 3.1 and Table 3.2. After device fabrication different environment condition like temperature  $T=300\text{k}$ ; illumination file was set as “AM1\_5G 1 sun.spe”. Then IV and QE calculations were set and put for calculation.

We simulated 6 ETLs and 6 HTLs as possible combinations with double perovskite solar cells. To achieve this, we fabricated multiple solar cell structures in SCAPS, 6 structures for each ETLs and HTLs. Parameters of these are given in **Error! Reference source not found.** and Table 3.2. For each of these cell structures simulation was performed and data was recorded as discussed in results section below.

Table 3.1:- various ETL parameters

Parameters (ETL)	IGZO	TiO <sub>2</sub>	ZnSe	ZnO	CeO <sub>2</sub>	WS <sub>2</sub>
E <sub>g</sub> (eV)	3.050	3.2	2.81	3.3	3.5	1.8
X (eV)	4.160	4	4.09	4	4.6	3.95
$\epsilon/\epsilon_0$	10	9	8.6	9	9	13.6
N <sub>c</sub> (cm <sup>-3</sup> )	5×10 <sup>18</sup>	2×10 <sup>18</sup>	2.2×10 <sup>18</sup>	3.7×10 <sup>18</sup>	1×10 <sup>20</sup>	1×10 <sup>18</sup>
N <sub>v</sub> (cm <sup>-3</sup> )	5×10 <sup>18</sup>	1.8×10 <sup>19</sup>	1.8×10 <sup>18</sup>	1.8×10 <sup>19</sup>	2×10 <sup>21</sup>	2.4×10 <sup>19</sup>
V <sub>e</sub> (cm S <sup>-1</sup> )	1×10 <sup>7</sup>	1×10 <sup>7</sup>	1×10 <sup>7</sup>	1×10 <sup>7</sup>	1×10 <sup>7</sup>	1×10 <sup>7</sup>
V <sub>h</sub> (cm S <sup>-1</sup> )	1×10 <sup>7</sup>	1×10 <sup>7</sup>	1×10 <sup>7</sup>	1×10 <sup>7</sup>	1×10 <sup>7</sup>	1×10 <sup>7</sup>
$\mu_e$ (cm <sup>2</sup> V <sup>-1</sup> S <sup>-1</sup> )	15	20	400	100	100	100
$\mu_h$ (cm <sup>2</sup> V <sup>-1</sup> S <sup>-1</sup> )	0.1	10	110	25	25	100
N <sub>D</sub> (cm <sup>-3</sup> )	1×10 <sup>17</sup>	9×10 <sup>16</sup>	1×10 <sup>15</sup>	1×10 <sup>18</sup>	1×10 <sup>21</sup>	1×10 <sup>18</sup>
N <sub>A</sub> (cm <sup>-3</sup> )	–	–	–	–	–	–
Defect density (cm <sup>-3</sup> )	1×10 <sup>15</sup>	1×10 <sup>15</sup>	1×10 <sup>15</sup>	1×10 <sup>15</sup>	1×10 <sup>15</sup>	1×10 <sup>15</sup>
REFERENCE	[25]–[27]	[25], [28], [29]	[30]	[25], [28], [31]	[25], [32]	[25], [28], [33]

Table 3.2:- Various HTL parameters

Parameters (HTL)	Spiro-OMeTAD	CuI	P3HT	Cu <sub>2</sub> O	PEDOT: PSS	CBTS
$E_g$ (eV)	3	3.1	1.7	2.2	1.6	1.9
$\chi$ (eV)	2.2	2.1	3.5	3.4	3.4	3.6
$\epsilon/\epsilon_0$	3	6.5	3	7.5	3	5.4
$N_C$ (cm <sup>-3</sup> )	$2.2 \times 10^{18}$	$2.8 \times 10^{19}$	$2 \times 10^{21}$	$2 \times 10^{19}$	$2.2 \times 10^{18}$	$2.2 \times 10^{18}$
$N_V$ (cm <sup>-3</sup> )	$1.8 \times 10^{19}$	$1 \times 10^{19}$	$2 \times 10^{21}$	$1 \times 10^{19}$	$1.8 \times 10^{19}$	$1.8 \times 10^{19}$
$V_e$ (cm S <sup>-1</sup> )	$1 \times 10^7$	$1 \times 10^7$	$1 \times 10^7$	$1 \times 10^7$	$1 \times 10^7$	$1 \times 10^7$
$V_h$ (cm S <sup>-1</sup> )	$1 \times 10^7$	$1 \times 10^7$	$1 \times 10^7$	$1 \times 10^7$	$1 \times 10^7$	$1 \times 10^7$
$\mu_e$ (cm <sup>2</sup> V <sup>-1</sup> S <sup>-1</sup> )	$2.1 \times 10^{-3}$	100	$1.8 \times 10^{-3}$	200	$4.5 \times 10^{-2}$	30
$\mu_h$ (cm <sup>2</sup> V <sup>-1</sup> S <sup>-1</sup> )	$2.16 \times 10^{-3}$	43.1	$1.86 \times 10^{-2}$	8600	$4.5 \times 10^{-2}$	10
$N_D$ (cm <sup>-3</sup> )	–	–	–	–	–	–
$N_A$ (cm <sup>-3</sup> )	$1 \times 10^{18}$	$1 \times 10^{18}$	$1 \times 10^{18}$	$1 \times 10^{18}$	$1 \times 10^{18}$	$1 \times 10^{18}$
Defect density (cm <sup>-3</sup> )	$1 \times 10^{15}$	$1 \times 10^{15}$	$1 \times 10^{15}$	$1 \times 10^{15}$	$1 \times 10^{15}$	$1 \times 10^{15}$
REFERENCE	[25], [28], [29], [34]	[25], [35]	[25], [28]	[25], [28], [36]	[25], [37], [38]	[25], [39]



Table 3.3:-Table for Parameters of (a) CBTS (b)perovskite layer (Cs<sub>2</sub> AgGaBr<sub>6</sub>) (c) ZnSe (d) FTO

Parameters	CBTS	Cs <sub>2</sub> AgGaBr <sub>6</sub>	ZnSe	FTO
Thickness (nm)	200	600	100	100
E <sub>g</sub> (eV)	1.9	1.420	2.81	3.5
χ (eV)	3.6	4.210	4.09	4.5
ε/ε <sub>0</sub>	5.4	3.600	8.6	9.00
N <sub>c</sub> (cm <sup>-3</sup> )	2.2 × 10 <sup>18</sup>	1.26 × 10 <sup>18</sup>	2.2 × 10 <sup>18</sup>	2.2 × 10 <sup>18</sup>
N <sub>v</sub> (cm <sup>-3</sup> )	1.8 × 10 <sup>19</sup>	1.73 × 10 <sup>18</sup>	1.8 × 10 <sup>18</sup>	1 × 10 <sup>19</sup>
V <sub>e</sub> (cm S <sup>-1</sup> )	1 × 10 <sup>7</sup>	1 × 10 <sup>7</sup>	1 × 10 <sup>7</sup>	1 × 10 <sup>7</sup>
V <sub>h</sub> (cm S <sup>-1</sup> )	1 × 10 <sup>7</sup>	1 × 10 <sup>7</sup>	1 × 10 <sup>7</sup>	1 × 10 <sup>7</sup>
μ <sub>e</sub> (cm <sup>2</sup> V <sup>-1</sup> S <sup>-1</sup> )	30	160.8	400	2 × 10 <sup>3</sup>
μ <sub>h</sub> (cm <sup>2</sup> V <sup>-1</sup> S <sup>-1</sup> )	10	4.800	110	2 × 10 <sup>3</sup>
N <sub>D</sub> (cm <sup>-3</sup> )	–	–	1 × 10 <sup>15</sup>	2 × 10 <sup>19</sup>
N <sub>A</sub> (cm <sup>-3</sup> )	1 × 10 <sup>18</sup>	–	–	–
Defect density (cm <sup>-3</sup> )	1 × 10 <sup>15</sup>	1.8 × 10 <sup>13</sup>	1 × 10 <sup>15</sup>	1 × 10 <sup>15</sup>
Reference	[25], [39]	[40], [41]	[30]	[40]

## 3.2 Cs<sub>2</sub>AgGaBr<sub>6</sub>

### 3.2.1 Structure

The device structure for the optimization of absorber layer is (FTO/ETL/Cs<sub>2</sub>AgInBr<sub>6</sub>/HTL/Au). Figure 3.2 shows device structure of optimized DPSC and its band gap alignment. Table 3.1 Table 3.2, and Table 3.3 shows the parameters of ETLs, HTLs, FTO, and absorber layer. The gold (Au) back contact is used in simulation. For Cs<sub>2</sub>AgInBr<sub>6</sub> some of the parameters used for simulation were obtained from previous works and others were calculated using the data available. For calculating density of state for valance and conduction bands (N<sub>v</sub> and N<sub>c</sub>) the given formula was used: -

$$N_{c/v} = 2 \left( \frac{2\pi k_B T m_{e/h}^*}{h^2} \right)^{\frac{3}{2}}$$

Here effective mass of electrons and holes i.e.,  $m_{e/h}^*$  differs from material to material. Using formula, we found values of,  $N_c = 1.26 \times 10^{18}$  and  $N_v = 1.73 \times 10^{18}$ . The dielectric constant was obtained using the following formula: -

$k = \frac{\epsilon}{\epsilon_0} = n^2$  where  $n$  = refractive index ( $n = 2.09$  [42]). We found value of dielectric constant as 4.368.

Band gap ( $E_g$ ) of material is taken as 1.47 eV[41]. The electron mobility and hole mobility are 89.4 and 3.30 ( $\text{cm}^2 \text{V}^{-1} \text{S}^{-1}$ ) respectively. The electron and hole thermal velocity is  $1 \times 10^7$  each.

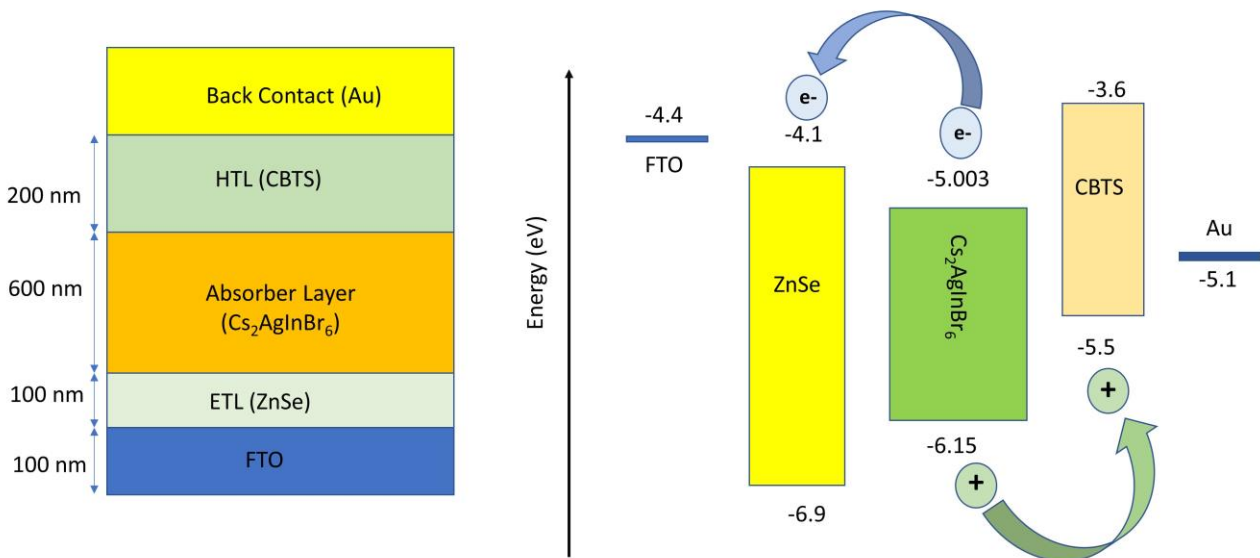


Figure 3.2:- Device structure and band gap alignment for  $\text{Cs}_2\text{AgInBr}_6$  based DPSC

### 3.2.2 DPSC design methodology: -

SCAPS software for 1-D designing was created by professor Marc Burgelman.[43], [44].For charge carriers (electrons and holes), SCAPS-1D can compute semiconductor equations such as continuity and Poisson's equations. Moreover, it can compute spectral response and current-voltage characteristics at various wavelengths specified by users. Additionally, this software's intrinsic capacity to imitate bulk defects and interface defects makes it commonly employed in the

numerical research of solar cells. Also, this simulation software has a standout feature that makes it a wise option for applications related to constructing solar cells. The Shockley-Read-Hall recombination model is used for the simulation, and illumination parameters are A.M 1.5G (Air Mass). Thus, a viable strategy for expanding the further growth of perovskite for solar applications is numerical PSC analysis using SCAPS-1D. The fundamental idea behind the tool is to solve continuity and Poisson's derivative equations using numerical differentiation and the Gummel type iteration method[45].

Table 3.4:- simulation parameters of initial DPSC layers.

Parameters	PEDOT:PSS	Cs <sub>2</sub> AgInBr <sub>6</sub>	IGZO	FTO
Thickness (nm)	200	600	100	100
E <sub>g</sub> (eV)	1.6	1.47	3.050	3.5
χ (eV)	3.4	4.10	4.160	4.5
ε/ε <sub>0</sub>	3	4.368	10	9.00
N <sub>C</sub> (cm <sup>-3</sup> )	2.2×10 <sup>18</sup>	1.26×10 <sup>18</sup>	5×10 <sup>18</sup>	2.2×10 <sup>18</sup>
N <sub>V</sub> (cm <sup>-3</sup> )	1.8×10 <sup>19</sup>	1.73×10 <sup>18</sup>	5×10 <sup>18</sup>	1×10 <sup>19</sup>
V <sub>e</sub> (cm S <sup>-1</sup> )	1×10 <sup>7</sup>	1×10 <sup>7</sup>	1×10 <sup>7</sup>	1×10 <sup>7</sup>
V <sub>h</sub> (cm S <sup>-1</sup> )	1×10 <sup>7</sup>	1×10 <sup>7</sup>	1×10 <sup>7</sup>	1×10 <sup>7</sup>
μ <sub>e</sub> (cm <sup>2</sup> V <sup>-1</sup> S <sup>-1</sup> )	4.5×10 <sup>-2</sup>	89.4	1.5	2×10 <sup>3</sup>
μ <sub>h</sub> (cm <sup>2</sup> V <sup>-1</sup> S <sup>-1</sup> )	4.5×10 <sup>-2</sup>	3.300	0.1	2×10 <sup>3</sup>
N <sub>D</sub> (cm <sup>-3</sup> )	–	-	1×10 <sup>17</sup>	2×10 <sup>19</sup>
N <sub>A</sub> (cm <sup>-3</sup> )	1×10 <sup>18</sup>	-	–	-
Defect density (cm <sup>-3</sup> )	1×10 <sup>15</sup>	1.8×10 <sup>14</sup>	1×10 <sup>15</sup>	1×10 <sup>15</sup>
Reference	[25], [38]	[23], [41], [42]	[25]–[27]	[40]

Table 3.5:- Simulation parameters of various HTLs

Parameters	CBTS	Spiro- OMeTAD	MASnBr <sub>3</sub>	CuO	PEDOT:PSS
Thickness (nm)	200	200	200	200	200
E <sub>g</sub> (eV)	1.9	3	2.15	1.51	1.6
χ (eV)	3.6	2.2	3.39	4.07	3.4
ε/ε <sub>0</sub>	5.4	3	8.2	18.1	3
N <sub>C</sub> (cm <sup>-3</sup> )	2.2 × 10 <sup>18</sup>	2.2 × 10 <sup>18</sup>	1 × 10 <sup>20</sup>	2.2 × 10 <sup>19</sup>	2.2 × 10 <sup>18</sup>
N <sub>V</sub> (cm <sup>-3</sup> )	1.8 × 10 <sup>19</sup>	1.8 × 10 <sup>19</sup>	1 × 10 <sup>18</sup>	5.5 × 10 <sup>20</sup>	1.8 × 10 <sup>19</sup>
V <sub>e</sub> (cm S <sup>-1</sup> )	1 × 10 <sup>7</sup>	1 × 10 <sup>7</sup>	1 × 10 <sup>7</sup>	1 × 10 <sup>7</sup>	1 × 10 <sup>7</sup>
V <sub>h</sub> (cm S <sup>-1</sup> )	1 × 10 <sup>7</sup>	1 × 10 <sup>7</sup>	1 × 10 <sup>7</sup>	1 × 10 <sup>7</sup>	1 × 10 <sup>7</sup>
μ <sub>e</sub> (cm <sup>2</sup> V <sup>-1</sup> S <sup>-1</sup> )	30	2.1 × 10 <sup>-3</sup>	1.6	100	4.5 × 10 <sup>-2</sup>
μ <sub>h</sub> (cm <sup>2</sup> V <sup>-1</sup> S <sup>-1</sup> )	10	2.16 × 10 <sup>-3</sup>	1.6	0.1	4.5 × 10 <sup>-2</sup>
N <sub>D</sub> (cm <sup>-3</sup> )	-	-	-	-	-
N <sub>A</sub> (cm <sup>-3</sup> )	1 × 10 <sup>18</sup>	1 × 10 <sup>18</sup>	1 × 10 <sup>18</sup>	1 × 10 <sup>18</sup>	1 × 10 <sup>18</sup>
Defect density (cm <sup>-3</sup> )	1 × 10 <sup>15</sup>	1 × 10 <sup>15</sup>	1 × 10 <sup>15</sup>	1 × 10 <sup>15</sup>	1 × 10 <sup>15</sup>
Reference	[25], [39]	[25], [28], [29], [34]	[46]	[25], [47]	[25], [38]

Table 3.6:- simulation parameters of various ETLs

<b>Parameters</b>	<b>ZnSe</b>	<b>TiO<sub>2</sub></b>	<b>IGZO</b>
<b>Thickness (nm)</b>	100	100	100
<b>E<sub>g</sub> (eV)</b>	2.81	3.2	3.050
<b>χ (eV)</b>	4.09	4	4.160
<b>ε/ε<sub>0</sub></b>	8.6	9	10
<b>N<sub>C</sub> (cm<sup>-3</sup>)</b>	2.2 × 10 <sup>18</sup>	2×10 <sup>18</sup>	5×10 <sup>18</sup>
<b>N<sub>V</sub> (cm<sup>-3</sup>)</b>	1.8 × 10 <sup>18</sup>	1.8×10 <sup>19</sup>	5×10 <sup>18</sup>
<b>V<sub>e</sub> (cm S<sup>-1</sup>)</b>	1 × 10 <sup>7</sup>	1×10 <sup>7</sup>	1×10 <sup>7</sup>
<b>V<sub>h</sub> (cm S<sup>-1</sup>)</b>	1 × 10 <sup>7</sup>	1×10 <sup>7</sup>	1×10 <sup>7</sup>
<b>μ<sub>e</sub> (cm<sup>2</sup> V<sup>-1</sup> S<sup>-1</sup>)</b>	400	20	1.5
<b>μ<sub>h</sub> (cm<sup>2</sup> V<sup>-1</sup> S<sup>-1</sup>)</b>	110	10	0.1
<b>N<sub>D</sub> (cm<sup>-3</sup>)</b>	1 × 10 <sup>15</sup>	9×10 <sup>16</sup>	1×10 <sup>17</sup>
<b>N<sub>A</sub> (cm<sup>-3</sup>)</b>	–	–	–
<b>Defect density (cm<sup>-3</sup>)</b>	1 × 10 <sup>15</sup>	1×10 <sup>15</sup>	1×10 <sup>15</sup>
<b>Reference</b>	[30]	[25], [28], [29]	[25]– [27]

## Chapter4 Results and Discussion

### 4.1 Cs<sub>2</sub>AgGaBr<sub>6</sub>

As discussed earlier we simulated multiple different Double perovskite solar cells using various ETLs and HTLs thereafter, the simulation data was recorded.

Table 4.1:- different cell structures and their simulation results

Device structure (FTO/ETL/Cs <sub>2</sub> AgGaBr <sub>6</sub> /HTL/Au)	Voc (volt)	Jsc(mA/cm <sup>2</sup> )	FF (%)	PCE (%)
FTO/TiO <sub>2</sub> /Cs <sub>2</sub> AgGaBr <sub>6</sub> /Spiro-OMeTAD/Au	1.24	29.16	81.79	29.63
FTO/ZnSe/Cs <sub>2</sub> AgGaBr <sub>6</sub> /Spiro-OMeTAD/Au	1.24	29.18	80.07	30.13
FTO/CeO <sub>2</sub> /Cs <sub>2</sub> AgGaBr <sub>6</sub> /Spiro-OMeTAD/Au	7.29	29.18	13.53	28.83
FTO/WS <sub>2</sub> /Cs <sub>2</sub> AgGaBr <sub>6</sub> /Spiro-OMeTAD/Au	1.24	29.17	81.68	29.62
FTO/ZnO/Cs <sub>2</sub> AgGaBr <sub>6</sub> /Spiro-OMeTAD/Au	1.24	28.93	82.92	29.79
FTO/IGZO/Cs <sub>2</sub> AgGaBr <sub>6</sub> /Spiro-OMeTAD/Au	1.24	29.14	82.88	29.99
FTO/TiO <sub>2</sub> /Cs <sub>2</sub> AgGaBr <sub>6</sub> /CBTS/Au	1.24	29.21	82.10	29.78
FTO/ZnSe/Cs <sub>2</sub> AgGaBr <sub>6</sub> /CBTS/Au	1.24	29.23	83.38	30.26
FTO/ZnO/Cs <sub>2</sub> AgGaBr <sub>6</sub> /CBTS/Au	1.24	29.21	83.35	30.24
FTO/CeO <sub>2</sub> /Cs <sub>2</sub> AgGaBr <sub>6</sub> /CBTS/Au	7.37	29.23	13.44	28.98
FTO/WS <sub>2</sub> /Cs <sub>2</sub> AgGaBr <sub>6</sub> /CBTS/Au	1.24	29.20	81.99	29.74
FTO/IGZO/Cs <sub>2</sub> AgGaBr <sub>6</sub> /CBTS/Au	1.24	29.28	83.25	29.95
FTO/TiO <sub>2</sub> /Cs <sub>2</sub> AgGaBr <sub>6</sub> /PEDOT: PSS/Au	1.24	29.30	79.77	29.04
FTO/CeO <sub>2</sub> /Cs <sub>2</sub> AgGaBr <sub>6</sub> /PEDOT: PSS/Au	1.99	29.25	50.27	29.33
FTO/WS <sub>2</sub> /Cs <sub>2</sub> AgGaBr <sub>6</sub> /PEDOT: PSS/Au	1.24	29.29	79.70	29.02
FTO/ZnO/Cs <sub>2</sub> AgGaBr <sub>6</sub> /PEDOT: PSS/Au	1.24	29.30	80.97	29.49
FTO/ZnSe/Cs <sub>2</sub> AgGaBr <sub>6</sub> /PEDOT: PSS/Au	1.24	29.33	80.97	29.51
FTO/IGZO/Cs <sub>2</sub> AgGaBr <sub>6</sub> /PEDOT: PSS/Au	1.24	29.07	80.80	29.17
FTO/TiO <sub>2</sub> /Cs <sub>2</sub> AgGaBr <sub>6</sub> /CuI/Au	1.24	29.09	83.05	30.02
FTO/CeO <sub>2</sub> /Cs <sub>2</sub> AgGaBr <sub>6</sub> /CuI/Au	9.10	29.18	10.63	28.25
FTO/WS <sub>2</sub> /Cs <sub>2</sub> AgGaBr <sub>6</sub> /CuI/Au	1.24	29.17	81.54	29.56
FTO/ZnO/Cs <sub>2</sub> AgGaBr <sub>6</sub> /CuI/Au	1.24	29.16	82.88	30.03
FTO/IGZO/Cs <sub>2</sub> AgGaBr <sub>6</sub> /CuI/Au	1.24	28.93	82.75	29.73
FTO/ZnSe/Cs <sub>2</sub> AgGaBr <sub>6</sub> /CuI/Au	1.24	29.18	82.89	30.05
FTO/TiO <sub>2</sub> /Cs <sub>2</sub> AgGaBr <sub>6</sub> /Cu <sub>2</sub> O/Au	1.24	29.17	82.16	29.78
FTO/CeO <sub>2</sub> /Cs <sub>2</sub> AgGaBr <sub>6</sub> /Cu <sub>2</sub> O/Au	7.54	29.20	13.15	28.96
FTO/ZnO/Cs <sub>2</sub> AgGaBr <sub>6</sub> /Cu <sub>2</sub> O/Au	1.24	29.18	83.41	30.24
FTO/IGZO/Cs <sub>2</sub> AgGaBr <sub>6</sub> /Cu <sub>2</sub> O/Au	1.24	28.95	83.30	29.94
FTO/WS <sub>2</sub> /Cs <sub>2</sub> AgGaBr <sub>6</sub> /Cu <sub>2</sub> O/Au	1.24	29.20	82.00	29.75
FTO/ZnSe/Cs <sub>2</sub> AgGaBr <sub>6</sub> /Cu <sub>2</sub> O/Au	1.24	29.20	83.44	30.26
FTO/TiO <sub>2</sub> /Cs <sub>2</sub> AgGaBr <sub>6</sub> /P3HT/Au	1.20	29.19	82.60	29.14

<b>FTO/ZnO/Cs<sub>2</sub>AgGaBr<sub>6</sub>/P3HT/Au</b>	1.22	29.19	82.41	29.57
<b>FTO/ZnSe/Cs<sub>2</sub>AgGaBr<sub>6</sub>/P3HT/Au</b>	1.20	29.21	83.90	29.61
<b>FTO/WS<sub>2</sub>/Cs<sub>2</sub>AgGaBr<sub>6</sub>/P3HT/Au</b>	1.21	29.21	81.93	29.12
<b>FTO/IGZO/Cs<sub>2</sub>AgGaBr<sub>6</sub>/P3HT/Au</b>	1.22	28.95	82.27	29.29
<b>FTO/CeO<sub>2</sub>/Cs<sub>2</sub>AgGaBr<sub>6</sub>/P3HT/Au</b>		29.21		26.56

recorded Device structure (FTO/ETL/Cs<sub>2</sub>AgGaBr<sub>6</sub>/HTL/Au) and their corresponding  $V_{oc}$  (volt),  $J_{sc}$ (mA/cm<sup>2</sup>), FF (%), PCE (%) Values obtained as a result of their respective simulations. The data for plotting various graphs and analysis were also recorded. After this analysis we found our optimized structure as FTO/ZnSe/Cs<sub>2</sub>AgGaBr<sub>6</sub>/CBTS/Au whose QE VS wavelength and  $J_{sc}$ -V curves were plotted as shown in Figure 4.3.

#### 4.1.1 Study of different ETL layers: -

The I-V AND ‘QE VS wavelength’ curves were obtained for 6 different ETL layers using data recorded in simulation and plotting the same in “Origin software” and the curves were studied Figure 4.1. It was observed ZnSe (Zinc Selenide) ETL showed the highest efficiency of 30.26%. Followed by ZnO with efficiency of 30.24. It was also observed that this highest efficiency coincided with CBTS as HTL layer.

ZnSe shows highest PCE which can be because of its, high electron mobility, suitable band gap alignment, high electron mobility and reduction in accumulation of charge at ETL/perovskite layer interface. Further ZnSe based devices shows better photostability because of greater ultraviolet light harvesting by ZnSe layer that results in efficiently avoiding intense UV-light exposure for perovskite film hence avoiding related degradation. [31, 19]

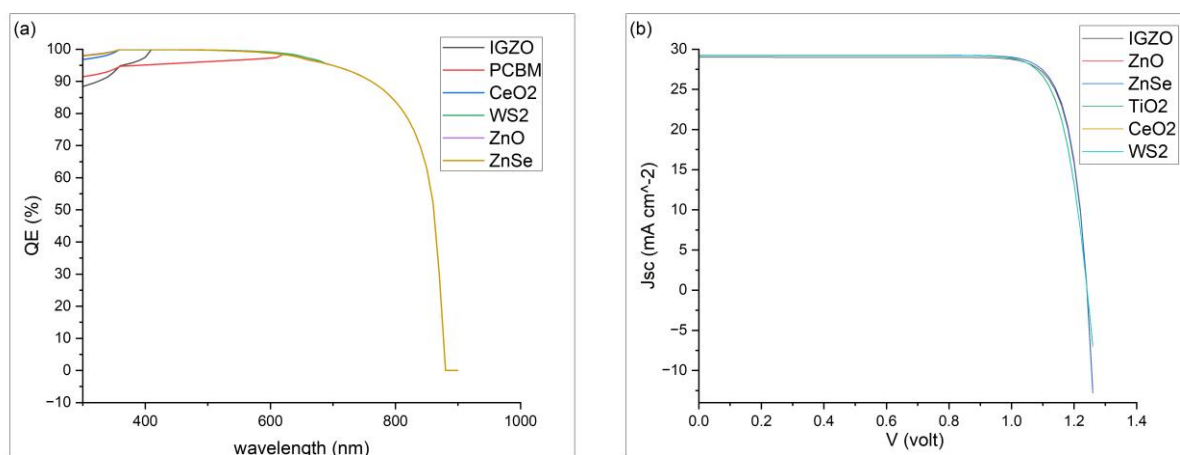


Figure 4.1 Graphs of (a)QE vs wavelength for various ETL layers (b) J-V curve for various ETL layers

#### 4.1.2 Study of HTL layers: -

The I-V AND ‘QE VS wavelength’ curves were obtained for 6 different HTL layers using data recorded in simulation and plotting the same in “Origin software” and the

curves were studied. It was observed CBTS (copper barium Thiostannate) layer has best efficiency of 30.26, followed by  $\text{Cu}_2\text{O}$  which also showed efficiency of 30.26 with ZnSe as ETL layer. But studied with different ETLs cell with CBTS as HTL is slightly better than  $\text{Cu}_2\text{O}$ . Because of suitable absorption coefficient and better electron affinity, CBTS as HTL gives better cell efficiency. [14, 29]. Thin film materials such as CBTS as HTL layer are also used over other common ones as they give better stability in air and are in abundance in earth. CBTS also offers tunable band gap and good light absorbing capacity. Non-centrosymmetric crystal structure with significant variation in CBTS atomic size provides suitable traits for improving the PCE of a solar cell. [14, 29]

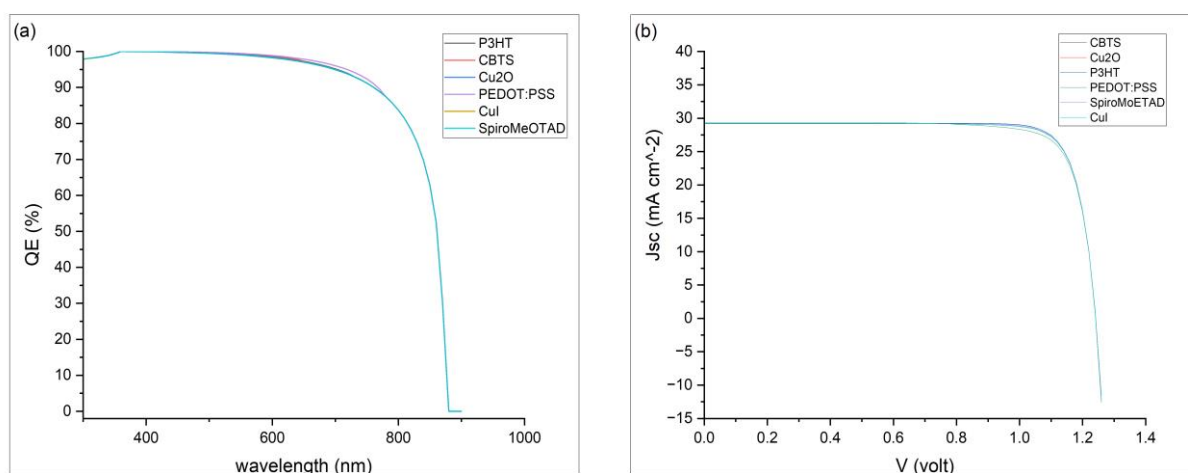


Figure 4.2:- Graphs of (a)QE vs wavelength for various HTL layers (b) J-V curve for various HTL layers

It was concluded that best combination for the cell was that of FTO/ZnSe/ $\text{Cs}_2\text{AgGaBr}_6$ /CBTS/Au with efficiency 30.26%. It therefore is also our optimized cell.

Table 4.1:- different cell structures and their simulation results

Device structure	$V_{oc}$	$J_{sc}(\text{mA}/\text{cm}^2)$	FF (%)	PCE
------------------	----------	---------------------------------	--------	-----



(FTO/ETL/Cs <sub>2</sub> AgGaBr <sub>6</sub> /HTL/Au)	(volt)		(%)	
FTO/TiO <sub>2</sub> /Cs <sub>2</sub> AgGaBr <sub>6</sub> /Spiro-OMeTAD/Au	1.24	29.16	81.79	29.63
FTO/ZnSe/Cs <sub>2</sub> AgGaBr <sub>6</sub> /Spiro-OMeTAD/Au	1.24	29.18	80.07	30.13
FTO/CeO <sub>2</sub> /Cs <sub>2</sub> AgGaBr <sub>6</sub> /Spiro-OMeTAD/Au	7.29	29.18	13.53	28.83
FTO/WS <sub>2</sub> /Cs <sub>2</sub> AgGaBr <sub>6</sub> /Spiro-OMeTAD/Au	1.24	29.17	81.68	29.62
FTO/ZnOCs <sub>2</sub> AgGaBr <sub>6</sub> /Spiro-OMeTAD/Au	1.24	28.93	82.92	29.79
FTO/IGZO/Cs <sub>2</sub> AgGaBr <sub>6</sub> /Spiro-OMeTAD/Au	1.24	29.14	82.88	29.99
FTO/TiO <sub>2</sub> /Cs <sub>2</sub> AgGaBr <sub>6</sub> /CBTS/Au	1.24	29.21	82.10	29.78
FTO/ZnSe/Cs <sub>2</sub> AgGaBr <sub>6</sub> /CBTS/Au	1.24	29.23	83.38	30.26
FTO/ZnO/Cs <sub>2</sub> AgGaBr <sub>6</sub> /CBTS/Au	1.24	29.21	83.35	30.24
FTO/CeO <sub>2</sub> /Cs <sub>2</sub> AgGaBr <sub>6</sub> /CBTS/Au	7.37	29.23	13.44	28.98
FTO/WS <sub>2</sub> /Cs <sub>2</sub> AgGaBr <sub>6</sub> /CBTS/Au	1.24	29.20	81.99	29.74
FTO/IGZO/Cs <sub>2</sub> AgGaBr <sub>6</sub> /CBTS/Au	1.24	29.28	83.25	29.95
FTO/TiO <sub>2</sub> /Cs <sub>2</sub> AgGaBr <sub>6</sub> /PEDOT: PSS/Au	1.24	29.30	79.77	29.04
FTO/CeO <sub>2</sub> /Cs <sub>2</sub> AgGaBr <sub>6</sub> /PEDOT: PSS/Au	1.99	29.25	50.27	29.33
FTO/WS <sub>2</sub> /Cs <sub>2</sub> AgGaBr <sub>6</sub> /PEDOT: PSS/Au	1.24	29.29	79.70	29.02
FTO/ZnO/Cs <sub>2</sub> AgGaBr <sub>6</sub> /PEDOT: PSS/Au	1.24	29.30	80.97	29.49
FTO/ZnSe/Cs <sub>2</sub> AgGaBr <sub>6</sub> /PEDOT: PSS/Au	1.24	29.33	80.97	29.51
FTO/IGZO/Cs <sub>2</sub> AgGaBr <sub>6</sub> /PEDOT: PSS/Au	1.24	29.07	80.80	29.17
FTO/TiO <sub>2</sub> /Cs <sub>2</sub> AgGaBr <sub>6</sub> /CuI/Au	1.24	29.09	83.05	30.02
FTO/CeO <sub>2</sub> /Cs <sub>2</sub> AgGaBr <sub>6</sub> /CuI/Au	9.10	29.18	10.63	28.25
FTO/WS <sub>2</sub> /Cs <sub>2</sub> AgGaBr <sub>6</sub> /CuI/Au	1.24	29.17	81.54	29.56
FTO/ZnO/Cs <sub>2</sub> AgGaBr <sub>6</sub> /CuI/Au	1.24	29.16	82.88	30.03
FTO/IGZO/Cs <sub>2</sub> AgGaBr <sub>6</sub> /CuI/Au	1.24	28.93	82.75	29.73
FTO/ZnSe/Cs <sub>2</sub> AgGaBr <sub>6</sub> /CuI/Au	1.24	29.18	82.89	30.05
FTO/TiO <sub>2</sub> /Cs <sub>2</sub> AgGaBr <sub>6</sub> /Cu <sub>2</sub> O/Au	1.24	29.17	82.16	29.78
FTO/CeO <sub>2</sub> /Cs <sub>2</sub> AgGaBr <sub>6</sub> /Cu <sub>2</sub> O/Au	7.54	29.20	13.15	28.96
FTO/ZnO/Cs <sub>2</sub> AgGaBr <sub>6</sub> /Cu <sub>2</sub> O/Au	1.24	29.18	83.41	30.24
FTO/IGZO/Cs <sub>2</sub> AgGaBr <sub>6</sub> /Cu <sub>2</sub> O/Au	1.24	28.95	83.30	29.94
FTO/WS <sub>2</sub> /Cs <sub>2</sub> AgGaBr <sub>6</sub> /Cu <sub>2</sub> O/Au	1.24	29.20	82.00	29.75
FTO/ZnSe/Cs <sub>2</sub> AgGaBr <sub>6</sub> /Cu <sub>2</sub> O/Au	1.24	29.20	83.44	30.26
FTO/TiO <sub>2</sub> /Cs <sub>2</sub> AgGaBr <sub>6</sub> /P <sub>3</sub> HT/Au	1.20	29.19	82.60	29.14
FTO/ZnO/Cs <sub>2</sub> AgGaBr <sub>6</sub> /P <sub>3</sub> HT/Au	1.22	29.19	82.41	29.57
FTO/ZnSe/Cs <sub>2</sub> AgGaBr <sub>6</sub> /P <sub>3</sub> HT/Au	1.20	29.21	83.90	29.61
FTO/WS <sub>2</sub> /Cs <sub>2</sub> AgGaBr <sub>6</sub> /P <sub>3</sub> HT/Au	1.21	29.21	81.93	29.12
FTO/IGZO/Cs <sub>2</sub> AgGaBr <sub>6</sub> /P <sub>3</sub> HT/Au	1.22	28.95	82.27	29.29
FTO/CeO <sub>2</sub> /Cs <sub>2</sub> AgGaBr <sub>6</sub> /P <sub>3</sub> HT/Au		29.21		26.56

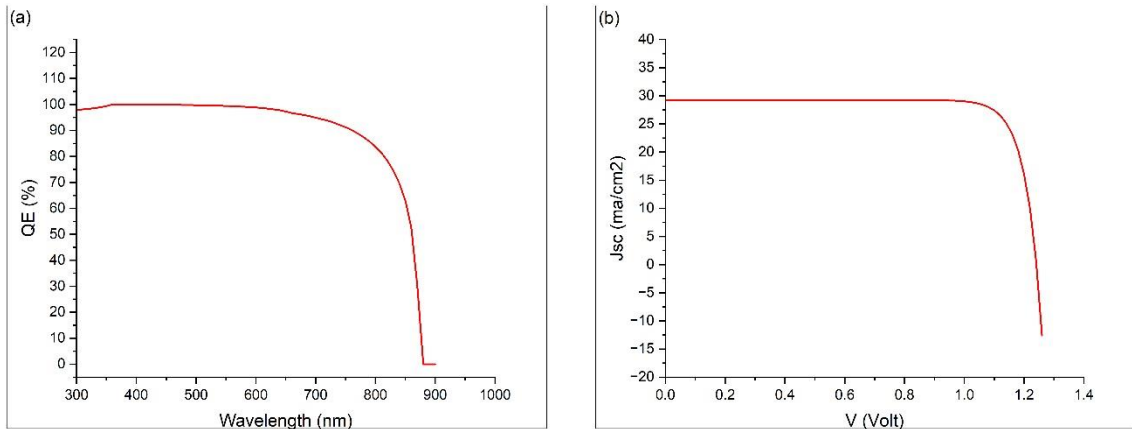


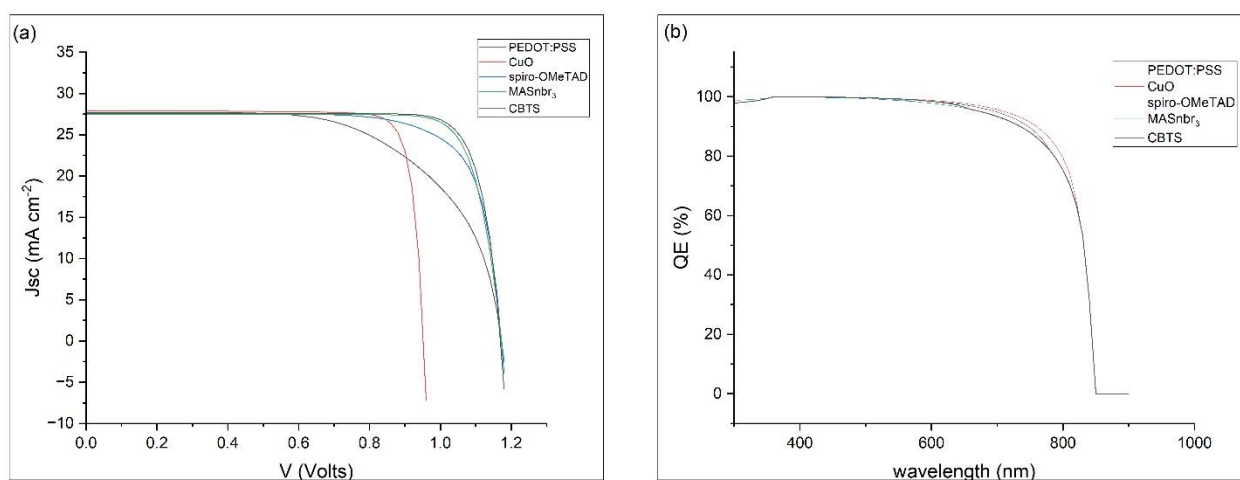
Figure 4.3:- Graphs of (a)QE vs wavelength for optimized cell (b) J-V curve for optimized cell structure

## 4.2 $\text{Cs}_2\text{AgInBr}_6$

### 4.2.1 Variation of HTLs and ETLs

We initially formed cell structure FTO/ IGZO / $\text{Cs}_2\text{AgInBr}_6$ /PEDOT:PSS/Au in SCAPS-1D using parameters as shown in ( Table 3.4). And obtained the cell efficiency of 19.79%. To increase the cell efficiency, we formed device structure with 5 HTLs (PEDOT:PSS, CuO, Spiro-OMeTAD,  $\text{MaSnBr}_3$ , CBTS) and 3 ETLs (IGZO,  $\text{TiO}_2$ , ZnSe) and studied their effect on DPSC parameters using data from SCAPS-1d simulations and plotting graphs on “origin-pro”. The simulation parameters of various HTLs and ETLs are shown in Table 3.5 and Table 3.6 respectively. The  $J_{sc}$  VS V curve and Q.E. VS wavelength curves are shown below in Figure 4.4 Figure 4.5, and Figure 4.6. The Q.E. (Quantum efficiency) is the ratio of number of carriers captured by the solar cell to number of photons incident on the solar cell with a specific energy. The Q.E. for a given wavelength is 1, when all photons at the wavelength are absorbed and the ensuing minority carriers are collected. The Q.E. is 0, when photon energy is less than band gap. Reflection and low diffusion length causes a reduction in overall Q.E. Reduction can also be accounted by near-surface recombination and reduced absorption at larger wavelengths. [43]

The more common device structure i.e., FTO/ TiO<sub>2</sub>/ Cs<sub>2</sub>AgInBr<sub>6</sub>/ Spiro-OMeTAD /Au gave efficiency of 24.34%. From the study we can conclude that DPSCs with ZnSe (Zinc Selenide) as ETL showed highest efficiency among the three ETL materials used, due to its wider band gap (Figure 3.2). ZnSe ETL based devices shows better photostability because of greater ultraviolet light harvesting by ZnSe layer that results in efficiently avoiding intense UV-light exposure for perovskite film hence avoiding related degradation. [30], [48] Whereas two HTLs i.e., MASnBr<sub>3</sub>, and CBTS (copper barium Thiostannate) showed highest efficiency of 26.97% and 26.90% with ZnSe. Since both vary little in efficiency and other parameters, we took CBTS as our HTL for optimization of absorber layer parameters. CBTS is a thin film material which offers tunable band gap and better light absorbing capacity. Non-centrosymmetric crystal structure with significant variation in CBTS atomic size provides suitable traits for improving the PCE of a solar cell. [25], [39] Therefore, in further parts of our study device structure is FTO/ZnSe/ Cs<sub>2</sub>AgInBr<sub>6</sub>/CBTS/Au for optimization of absorber layer. Simulation



parameters of optimized layers are shown in tables above. Suitable band alignment diagram and device structure for further device optimization is shown in Figure 3.2.

Figure 4.4:- graphs of (a)  $J_{sc}$  VS Voltage (b) QE vs wavelength with ZnSe as ETL and varying HTLs

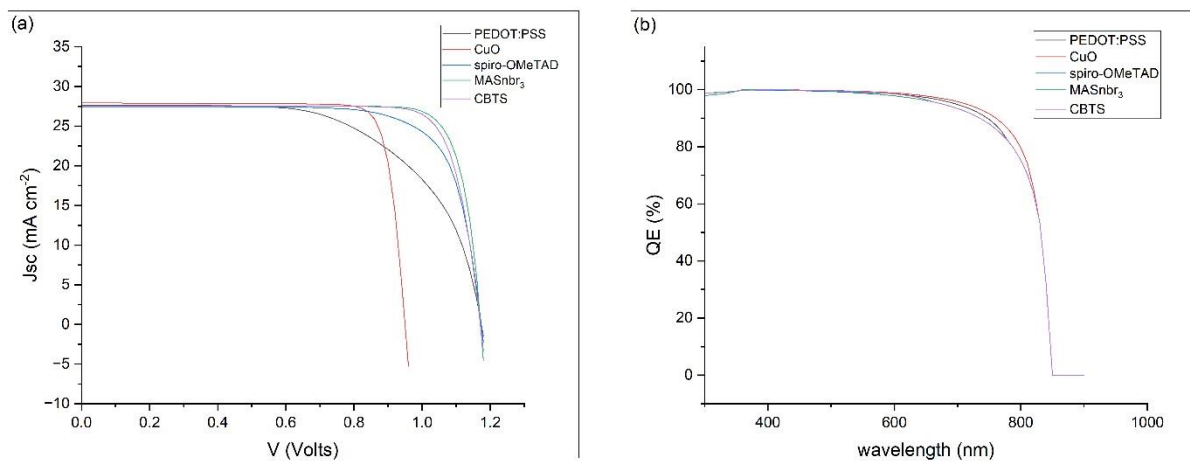


Figure 4.5:- graphs of (a)  $J_{sc}$  VS Voltage (b) QE vs wavelength with  $\text{TiO}_2$  as ETL and varying HTLs

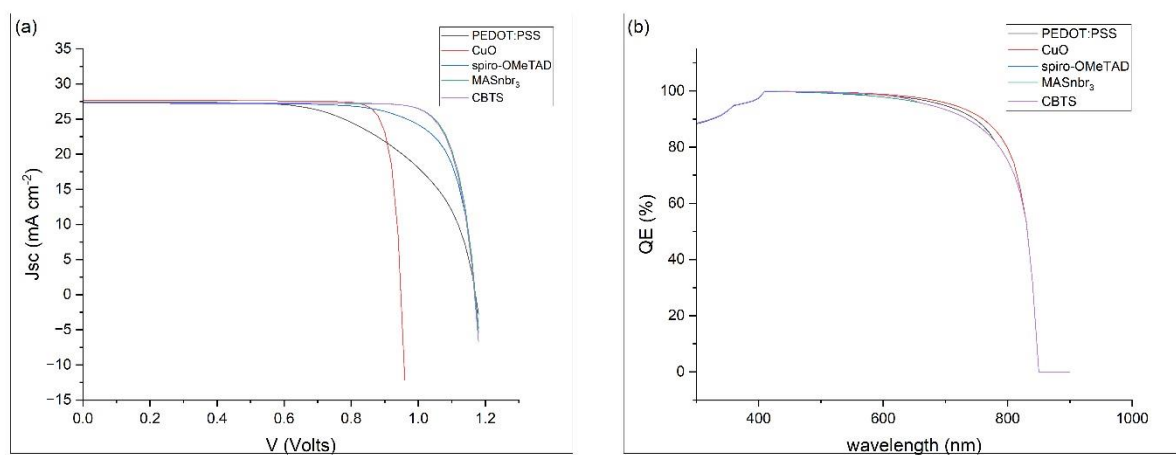


Figure 4.6:- graphs of (a)  $J_{sc}$  VS Voltage (b) QE vs wavelength with IGZO as ETL and varying HTLs

Table 4.2:- Different cell structure and their simulation results

DEVICE STRUCTURE	FF (%)	V <sub>oc</sub> (volt)	J <sub>sc</sub> (mA cm <sup>-2</sup> )	PCE (%)
FTO/ZnSe/Cs <sub>2</sub> AgInBr <sub>6</sub> /CBTS/Au	83.49	1.17	27.54	26.90
FTO/ZnSe/ Cs <sub>2</sub> AgInBr <sub>6</sub> /MASnBr <sub>3</sub> /Au	83.69	1.17	27.49	26.97
FTO/ZnSe/ Cs <sub>2</sub> AgInBr <sub>6</sub> /spiro-OMeTAD/Au	75.57	1.17	27.44	24.34
FTO/ZnSe/ Cs <sub>2</sub> AgInBr <sub>6</sub> /CuO/Au	88.5	0.95	27.89	22.75
FTO/ZnSe/ Cs <sub>2</sub> AgInBr <sub>6</sub> /PEDOT: PSS/Au	62.23	1.17	27.49	20.19
FTO/IGZO/ Cs <sub>2</sub> AgInBr <sub>6</sub> /CBTS/Au	83.30	1.16	27.28	26.56
FTO/IGZO/ Cs <sub>2</sub> AgInBr <sub>6</sub> /MASnBr <sub>3</sub> /Au	83.46	1.17	27.24	26.61
FTO/IGZO/ Cs <sub>2</sub> AgInBr <sub>6</sub> /spiro-OMeTAD /Au	75.96	1.170	27.21	24.21
FTO/IGZO/ Cs <sub>2</sub> AgInBr <sub>6</sub> /CuO/Au	86.84	0.94	27.66	22.82
FTO/IGZO/ Cs <sub>2</sub> AgInBr <sub>6</sub> /PEDOT: PSS/Au	61.67	1.17	27.40	19.79
FTO/TiO <sub>2</sub> / Cs <sub>2</sub> AgInBr <sub>6</sub> / CBTS /Au	82.22	1,17	27.52	26.50
FTO/TiO <sub>2</sub> / Cs <sub>2</sub> AgInBr <sub>6</sub> / MASnBr <sub>3</sub> /Au	82.41	1.17	27.63	26.56
FTO/TiO <sub>2</sub> / Cs <sub>2</sub> AgInBr <sub>6</sub> / spiro-OMeTAD /Au	75.57	1.17	27.44	24.34
FTO/TiO <sub>2</sub> / Cs <sub>2</sub> AgInBr <sub>6</sub> /CuO/Au	85.04	0.95	27.89	22.55
FTO/TiO <sub>2</sub> / Cs <sub>2</sub> AgInBr <sub>6</sub> /PEDOT: PSS/Au	61.61	1.17	27.63	19.99

#### 4.2.2 Optimization of Absorber layer Defect density (N<sub>t</sub>)

Batch calculations were Carried out in SCAPS-1D for studying the effect of change in N<sub>t</sub> of Cs<sub>2</sub>AgInbr<sub>6</sub>- layer on the PCE and other parameters of Cs<sub>2</sub>AgInbr<sub>6</sub> solar cell. Defect Density, N<sub>t</sub> was varied in steps of 10<sup>1</sup> at a constant thickness of 600 nm. All other parameters of ETL, HTL, FTO and absorber layers were kept same as mentioned in Table 3.4 we observed that with increase of N<sub>t</sub>, efficiency of DPSC decreased. Only slight variation in efficiency was seen below Defect Density N<sub>t</sub> = 10<sup>10</sup> cm<sup>-3</sup> at which point efficiency of 37.21%. above this value of defect density

efficiency of solar cell decreases sharply and comes down to 24.65% at  $1.3 \times 10^{15}$  and to 8.71% at  $1.3 \times 10^{18}$ .

$N_t$  in the active layer is a critical variable that has a big impact on efficiency of device. High defect concentration means recombination is also high because of pinholes generation, greater degradation rate of film, reduction in stability and

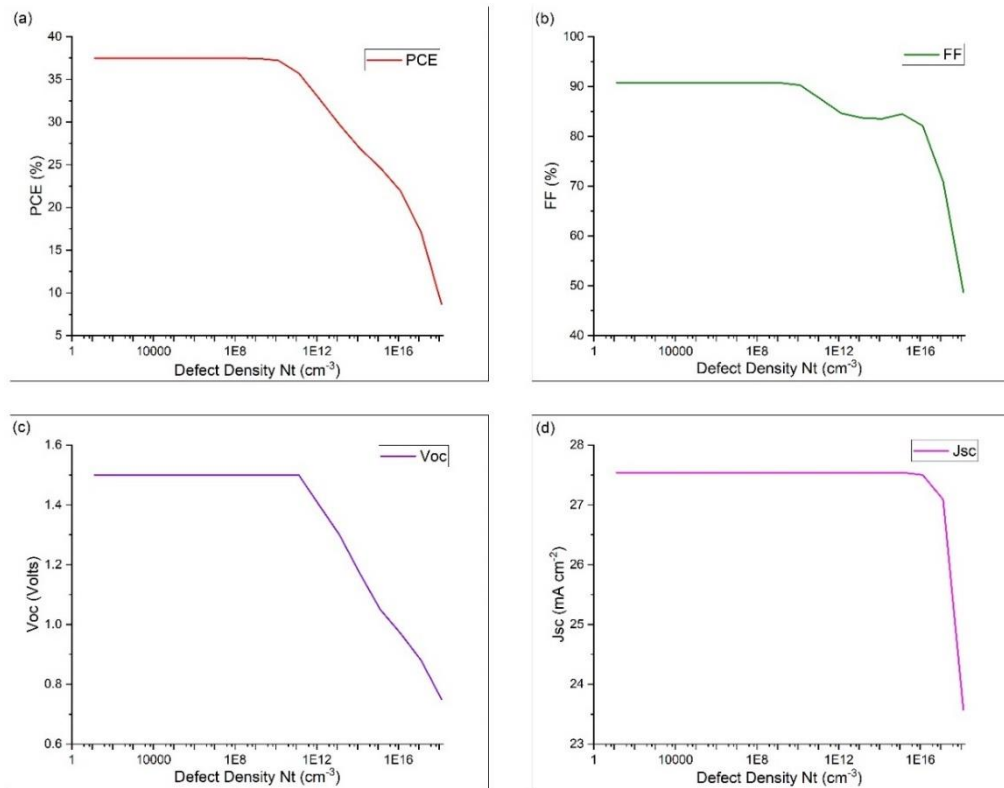


Figure 4.7:- graph showing change in various DPSC parameters as a function of defect density,  $N_t$

overall reduction in device performance.

### 4.2.3 Optimization of thickness of absorber layer

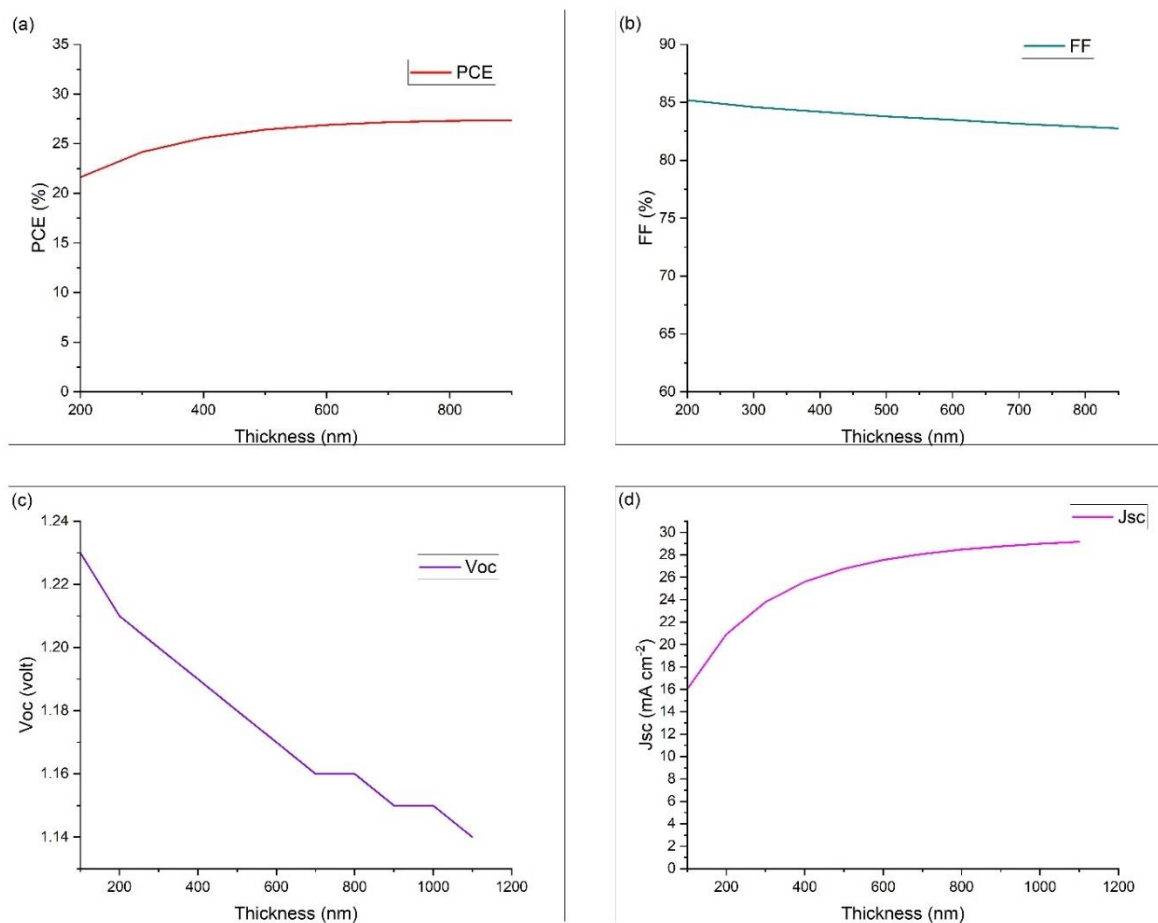


Figure 4.8:- graph showing change in various DPSC parameters as a function of thickness of  $\text{Cs}_2\text{AgInBr}$  layer

Batch calculations were Carried out in SCAPS-1D for studying effect of thickness of absorbing layer on efficiency and other parameters of  $\text{Cs}_2\text{AgInBr}_6$  solar cell. Thickness was varied in steps of 100nm at a constant defect density of  $10^{14}$ . all other parameters of ETL, HTL, FTO and absorber layers were kept same as mentioned in, tables above. It was seen that as thickness increased, efficiency also increased because at low thickness photons could not absorb light adequately. but it started decreasing after 1000 nm due to recombination of carriers occur for thick film. Maximum efficiency of 27.36% was observed at 900nm and 1000nm. Values of fill factor decreases from 85.88 at 100nm to 82.34 at 1000nm and slight decline in values of voltage could be observed. Current density values increase with increase in thickness. Starting from 16.01 at 100 nm, it rises to 27.99 at 1000K.

Active layer's thickness is key factor for maximising the PCE of DPSC. To maximise current density and reduce the reverse saturation current, it should be properly selected. Reduced electric field has an impact on the recombination behaviour of charge carriers, which results in an efficiency drop, in thicker absorber layers [47]. FF is inversely related to thickness of absorber because series resistance increases and power dissipation internally increases, in thick absorbing layer. There is also a simultaneous decrease in  $V_{oc}$  with thickness( Figure 4.8) because as dark saturation current increases there is simultaneous increase in recombination of charge carrier.[30]

#### 4.2.4 Effect of Temperature

We have varied temperature in range 200 to 800K to investigate the temperature's

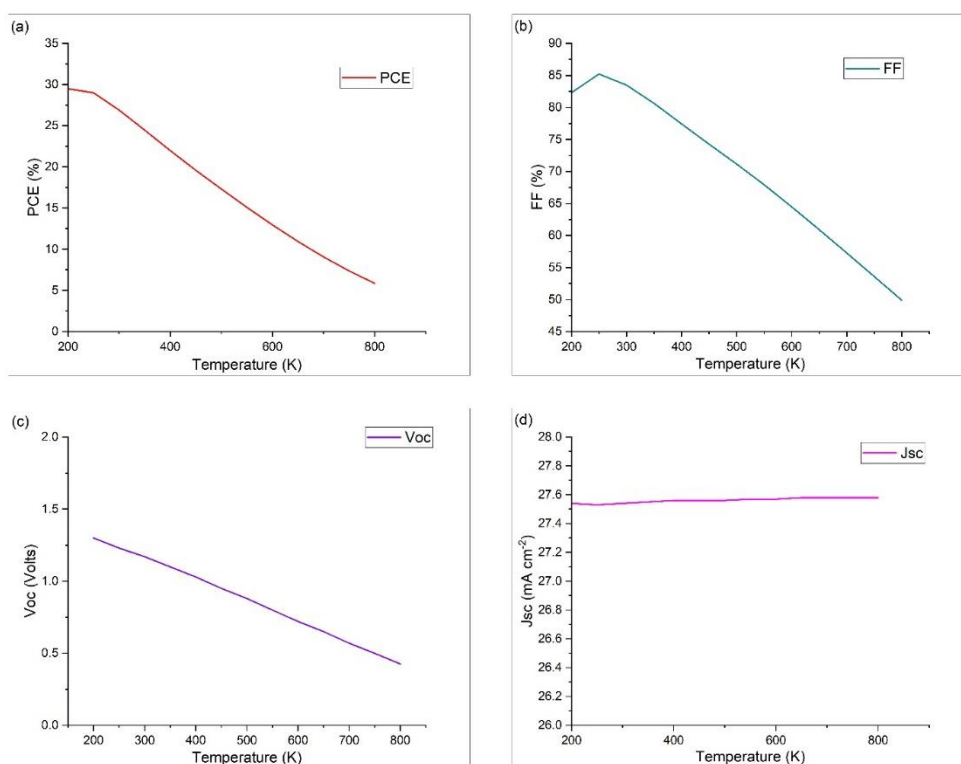


Figure 4.9:- graph showing in various DPSC parameters as a function of Temperature

effect on four parameters of DPSC with the view of interrogating the thermal stability of device. We observed the decrease in PCE, FF,  $V_{oc}$  and slight increase in



current density. Maximum efficiency of 29.49 is calculated at 200K and minimum of 5.86 at 800 K. FF initially increases then decrease...we obtain Max value of 85.21 at 250K and then it reduces to 49.89 Minimum value.

The device's performance is significantly influenced by the operating temperature. Solar panels are typically installed outside and frequently function at temperatures above 300 K. According to reports, raising the temperature makes structures under more strain and stress which results in increase interfacial defects, disorder, and low interconnectivity in layers. Temperature rise also impacts the hole and electron mobilities and carrier concentration, which lowers the PSCs' efficiency. Increasing temperature also causes a minor rise in  $J_{sc}$  (Figure 4.9)Figure 4.9:- graph showing in various DPSC parameters as a function of Temperature, which is a result of reduced energy band gap and creation of additional electron-hole pairs. The drop in  $V_{oc}$  with temperature rise (Figure 4.9), may be explained by more interfacial defects created along with

#### **4.2.5 Optimization of Electron affinity: -**

For the optimization of electron affinity, we changed the absorber layer's electron affinity from 3.5 eV to 4.5 eV. keeping all other properties of all layers of the solar cell with structure FTO/ZnSe/  $Cs_2AgInBr_6$  /CBTS/Au same. We collected and plotted the data using “origin” software and studied the DPSC parameters as shown in Figure 4.10.

We found optimum value of election affinity can be taken as 4.1 eV as determined from graph with efficiency 26.9%. the graphical study shows that PCE, FF,  $V_{oc}$ , and  $J_{sc}$  show stability with electron affinity between 3.6 and 4.3 with only slight and stable variation in these parameters.

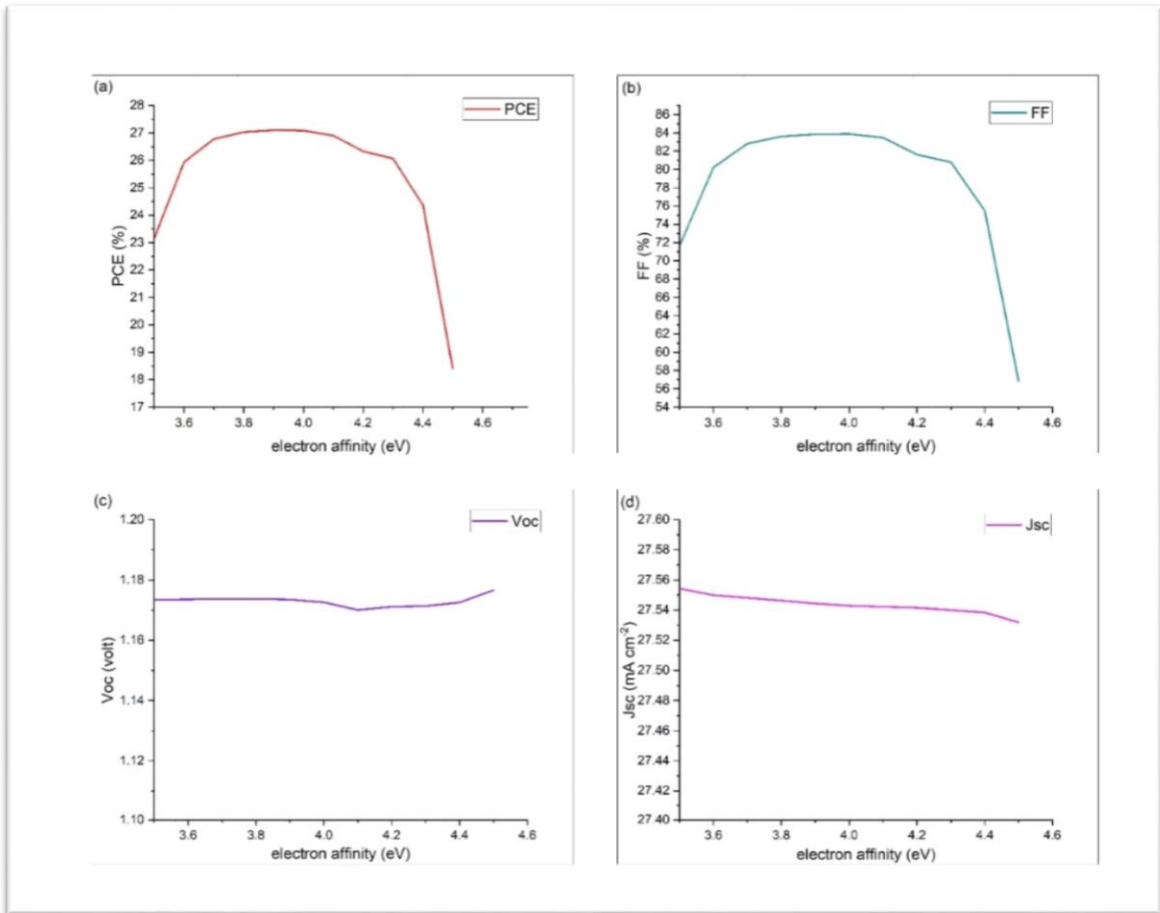


Figure 4.10:- graph showing change in various DPSC parameters as a function of electron affinity

### 4.3 CBTS HTL: -

Copper Barium Thiostannate (CBTS) is a ternary compound composed of copper (Cu), barium (Ba), sulphur (S), and tin (Sn). It is known for its p-type semiconductor properties, making it suitable for use as an HTL in solar cells.

Advantages of CBTS as an HTL material:

- 1 High Hole Mobility: CBTS exhibits high hole mobility, enabling efficient transport of positive charge carriers (holes) within the material. This characteristic facilitates the holes-extraction from the active layer as well as their movement towards the electrode, contributing to improved charge transport and device performance.

2      **Suitable Energy Level Alignment:** CBTS can be engineered to have energy levels that align well with the active layer of the photovoltaic device. This alignment ensures efficient charge extraction and reduces energy losses at the HTL/active layer interface.

3      **Stability:** CBTS offers good chemical and thermal stability, which is critical for long-term performance and reliability of the photovoltaic device.

4      **Solution Processability:** CBTS can be processed from solution, allowing for reduced-cost and scalable fabrication techniques like spin-coating or inkjet printing. This solution processability enhances the potential for large-scale manufacturing of solar cells.

5      It's important to note that while CBTS shows promise as an HTL material, its application in solar cells is undergoing research. The specific device architectures, optimization techniques, and performance characteristics of CBTS-based solar cells may vary depending on the research and development efforts in the field.

#### **4.4 HTL has larger impact than ETL on solar cell: -**

Yes, the choice and properties of the hole transport layer (HTL) has significant impact on the overall efficiency of a solar cell, often more so than the electron transport layer (ETL). Here's why:

1.      **Charge Extraction:** The HTL is responsible for extracting holes generated in the active layer of the solar cell and transporting them to the electrode. Efficient hole extraction is crucial to minimize carrier recombination and maximize the overall device efficiency. A well-designed HTL with high hole mobility and suitable energy level alignment can facilitate efficient charge extraction and reduce losses at the HTL/active layer interface.

2.      **Interface Recombination:** The interface between the HTL and the active layer is a critical region where charge carrier recombination can occur. A properly selected HTL can reduce interfacial recombination by providing a favourable energy level alignment, preventing charge carriers from being trapped or lost at the interface.

3.      **Carrier Transport:** The HTL's ability to efficiently transport holes through the device plays a crucial role in minimizing carrier losses and improving the collection efficiency. High hole mobility within the HTL ensures that the generated charge

carriers can move freely towards the electrode without significant recombination or trapping events.

4. Contact Resistance: The electrical contact between the HTL and the electrode influences the overall device performance. A good HTL should provide a low-resistance contact, enabling efficient charge transfer and minimizing energy losses.

While the ETL also plays a crucial role in charge extraction and transport, the HTL is often considered more critical due to its direct interaction with the active layer and its impact on hole extraction, interface recombination, and carrier transport. However, both the HTL and ETL need to be carefully designed and optimized to achieve high device efficiency.

It's important to note that the efficiency of a PSC is a complex interplay of multiple factors, including the active layer material, device architecture, and overall device engineering. The HTL and ETL must work synergistically to facilitate efficient charge extraction and transport throughout the device. Therefore, optimizing both the HTL and ETL is essential for maximizing the solar cell's overall performance.

## Chapter5 Conclusion

### 5.1 Cs<sub>2</sub>AgGaBr<sub>6</sub>: -

As a result of the discussion above, we may say that Cs<sub>2</sub>AgBiBr<sub>6</sub> as a double perovskite material is alternate for Pb-based PSCs with a very high efficiency in theoretical simulations. We studied effects of various HTL and ETL on the efficiency of Cs<sub>2</sub>AgBiBr<sub>6</sub> based DPSC. We took 6 different ETLs and 6 HTLs which led to various combination of solar cell structures. All of these solar cell structures were studied and their solar cell parameters like PCE were recorded. In this study we found CBTS as the best HTL and ZnSe as best ETL. Combination of these two layers makes following solar cell structure FTO/ZnSe/Cs<sub>2</sub>AgGaBr<sub>6</sub>/CBTS/Au, which gave the efficiency of 30.26%. This is among the best at a lower thickness of 600 nm. We also carried out graphical study of various ETL and HTL based solar cells to conclude the same. Our study establishes the work for application of CBTS and ZnSe as future HTLs and ETLs respectively for study and manufacturing of solar cells. Our study can help the future practical works on Cs<sub>2</sub>AgBiBr<sub>6</sub> which is seen as an excellent material for photovoltaics research and manufacturing, in absence of any practical work on the material our studies may be considered as predictions.

### 5.2 Cs<sub>2</sub>AgInBr<sub>6</sub>: -

From the above discussion we can conclude that Cs<sub>2</sub>AgInBr<sub>6</sub> is a promising DPSC and has excellent potential for application in solar cell industry. Optimization of defect density suggest that PCE of solar cell remains constant until  $10^{10}$  and then decreases with increase in defect density. Also, PCE increased with increase in thickness and became maximum at 900 and 1000 nm with a value of 27.36% after which it started decreasing. The effect of temperature was studied and PCE decreased steadily with increase in temperature, in our study PCE was maximum at 200 K with a value of 29.49 ( $N_t = 10^{14}$ ) and it was 26.9 at 300 K. We also studied combination of 2 HTLs and 2 ETLs in the cell structure and its efficiency. Finally, the optimised cell FTO/ZnSe/Cs<sub>2</sub>AgInBr<sub>6</sub>/CBTS/Au with optimized parameters got us efficiency of 26.90% and the FTO/ZnSe/Cs<sub>2</sub>AgInBr<sub>6</sub>/MASnBr<sub>3</sub>/Au cell showed highest efficiency of 26.97% with optimized parameters.

## APPENDICES

### APPENDIX 1 PLAGIARISM REPORT



Similarity Report ID: oid:27535:36490168

PAPER NAME

**thesis draft 1 (AutoRecovered) 2.docx**

WORD COUNT

**10769 Words**

CHARACTER COUNT

**62132 Characters**

PAGE COUNT

**55 Pages**

FILE SIZE

**5.6MB**

SUBMISSION DATE

**May 30, 2023 11:33 AM GMT+5:30**

REPORT DATE

**May 30, 2023 11:34 AM GMT+5:30**

#### ● 9% Overall Similarity

The combined total of all matches, including overlapping sources, for each database.

- 6% Internet database
- Crossref database
- 7% Submitted Works database
- 4% Publications database
- Crossref Posted Content database

#### ● Excluded from Similarity Report

- Bibliographic material
- Manually excluded text blocks
- Small Matches (Less than 8 words)

9% Overall Similarity

Top sources found in the following databases:

- 6% Internet database
- 4% Publications database
- Crossref database
- Crossref Posted Content database
- 7% Submitted Works database

TOP SOURCES

The sources with the highest number of matches within the submission. Overlapping sources will not be displayed.

1	dokumen.pub	Internet	<1%
2	Higher Education Commission Pakistan on 2022-09-21	Submitted works	<1%
3	dspace.dtu.ac.in:8080	Internet	<1%
4	Ashish D. Rana, Indrajit D. Pharne, Kshitij Bhargava. "Numerical simula...	Crossref	<1%
5	iopscience.iop.org	Internet	<1%
6	National Institute of Technology, Raipur on 2023-03-23	Submitted works	<1%
7	repo.ust.edu.sd:8080	Internet	<1%
8	hindawi.com	Internet	<1%

9	nith on 2023-05-18	Submitted works	<1%
10	researchgate.net	Internet	<1%
11	science.gov	Internet	<1%
12	Kibbou Moussa, Haman Zakaryae, Khossossi Nabil, Ismail Essaoudi, A...	Crossref	<1%
13	M. Belarbi, O. Zeggai, S. Louhibi-Fasila. "Numerical study of Methyam...	Crossref	<1%
14	Sheikh Rashed Al Ahmed, Mostafizur Rahaman, Adil Sunny, Sabrina Ra...	Crossref	<1%
15	tel.archives-ouvertes.fr	Internet	<1%
16	Al Akhawayn University in Ifrane on 2021-12-18	Submitted works	<1%
17	University of New South Wales on 2020-11-16	Submitted works	<1%
18	mzuir.inflibnet.ac.in	Internet	<1%
19	Higher Education Commission Pakistan on 2014-07-17	Submitted works	<1%
20	Shri Vishwakarma Skill University on 2021-05-31	Submitted works	<1%

21	T. Bendib, H. Bencherif, M.A. Abdi, F. Meddour, L. Dehimi, M. Chahdi. "...	Crossref	<1%
22	coursehero.com	Internet	<1%
23	Milua Masikini, Samuel Mkiehlane, Emmanuel Iwuoha. "Synthesis and ...	Crossref	<1%
24	tudr.thapar.edu:8080	Internet	<1%
25	Indian Institute of Technology IIT Palakkad on 2023-05-04	Submitted works	<1%
26	Institute of Infrastructure Technology Research and Management - IIT...	Submitted works	<1%
27	University of Bolton on 2023-05-12	Submitted works	<1%
28	backoffice.biblio.ugent.be	Internet	<1%
29	nanopdf.com	Internet	<1%
30	theses.hal.science	Internet	<1%
31	Khulna University of Engineering & Technology on 2023-02-20	Submitted works	<1%
32	M. Bilal Faheem, Bilawal Khan, Chao Feng, M. Umar Farooq, Fazal Razl...	Crossref	<1%

33	Prema Mahajan, Ram Datt, Wing Chung Tsoi, Vinay Gupta, Amit Tomar, ...	Crossref	<1%
34	Rui Wang, Jingjing Xue, Lei Meng, Jin-Wook Lee et al. "Caffeine Improv...	Crossref	<1%
35	repository.tudelft.nl	Internet	<1%
36	spiedigitallibrary.org	Internet	<1%
37	Chandani Dubey, Deepak Kumar Jarwal, Hemant Kumar, Yogesh Kuma...	Crossref	<1%
38	Chittagong University of Engineering and Technology on 2019-08-27	Submitted works	<1%
39	Gulf University on 2015-10-03	Submitted works	<1%
40	Neelima Singh, Alpana Agarwal, Mohit Agarwal. "Performance evaluati...	Crossref	<1%
41	Shambhavi Rai, B.K. Pandey, D.K. Dwivedi. "Designing hole conductor f...	Crossref	<1%
42	Shivani Chauhan, Rachna Singh. "Analysis of absorber layer for wide-b...	Crossref	<1%
43	University of Hertfordshire on 2021-06-21	Submitted works	<1%
44	Vaibhava Srivastava, R K Chauhan, Pooja Lohia. "Theoretical study of L...	Crossref	<1%

45	e-archivo.uc3m.es	Internet	<1%
46	espace.library.uq.edu.au	Internet	<1%
47	geomgrav.fi.ut.ee	Internet	<1%
48	link.springer.com	Internet	<1%
49	pure.rug.nl	Internet	<1%
50	freepatentsonline.com	Internet	<1%
51	American University of the Middle East on 2020-12-03	Submitted works	<1%
52	Bernabé Marí Soucase, Faisal Baig, Yousaf Hameed Khattak, Erika Veg...	Crossref	<1%
53	Gagandeep, Mukhtiyar Singh, Ramesh Kumar, Vinamrita Singh. "Investi...	Crossref	<1%
54	Lalsingh Guguloth, Kuldeep Singh, V.S. Reddy Channu, Kusum Kumari. ...	Crossref	<1%
55	M. Khalid Hossain, Mirza Humaun Kabir Rubel, G. F. Ishraque Toki, Inte...	Crossref	<1%
56	Md. Helal Miah, Md. Bulu Rahman, Fatema Khatun, Mayeen Uddin Kha...	Crossref	<1%

57	Nanyang Technological University on 2023-04-16	Submitted works	<1%
58	National Institute Of Technical Teachers' Training & Research on 2022-...	Submitted works	<1%
59	National Institute of Technology, Raipur on 2022-01-20	Submitted works	<1%
60	P. Arockia Michael Mercy, K.S. Joseph Wilson. "Development of enviro...	Crossref	<1%
61	Sadia Ameen, M. Shaheer Akhtar, Hyung-Shik Shin, Mohammad Khaja ...	Crossref	<1%
62	Universiti Kebangsaan Malaysia on 2023-05-17	Submitted works	<1%
63	catalog.lib.kyushu-u.ac.jp	Internet	<1%
64	engagedscholarship.csuohio.edu	Internet	<1%
65	etd.uwc.ac.za	Internet	<1%
66	m.scirp.org	Internet	<1%
67	mdpi-res.com	Internet	<1%
68	jos.ac.cn	Internet	<1%

69	thefreelibrary.com	Internet	<1%
----	--------------------	----------	-----

● Excluded from Similarity Report

- Bibliographic material
- Manually excluded text blocks
- Small Matches (Less than 8 words)

EXCLUDED TEXT BLOCKS

A DISSERTATION

dspace.dtu.ac.in:8080

under the guidance of Dr

dspace.dtu.ac.in:8080

hereby certify that the work which is presented in the Dissertation Project-II/Resea...

dspace.dtu.ac.in:8080

in fulfilment of the requirement for the award of the degree of Master of Science in ...

dspace.dtu.ac.in:8080

has been

dspace.dtu.ac.in:8080

SUPERVISOR CERTIFICATE to the best of my knowledge

dspace.dtu.ac.in:8080

DELHI TECHNOLOGICAL UNIVERSITY(Formerly Delhi College of Engineering)Bawa...

dspace.dtu.ac.in:8080



## APPENDIX 2 ABSTRACT ACCEPTANCE MAIL (PAPER 1)

## Urgent: ICAMET 2023 – LAST DAY OF REGISTRATION (NO ON-SITE REGISTRATION)

External Inbox



International Conference Apr 25

to bcc: me



Dear Participants,

Greetings!!

Thank you for the interest shown in ICAMET-2023 and submitting your abstract for presentation. We are pleased to inform you that **abstract** of your paper has been **accepted for presentation** during the International Conference on Advanced Materials for Emerging Technologies (ICAMET-2023) to be held at **APJ-11, Netaji Subhas University of Technology, New Delhi**.

**Due to overwhelming response, the accepted abstract of registered candidates will only be printed in the Abstract Book.**

**Please complete the registration process by Today (25th April 2023).**

**No On-site registration will be allowed.**

**Please complete the following google form also.**


Google Form Link: <https://forms.gle/vxHFLzX9r8pAx2q17>

We look forward to welcoming you at Netaji Subhas University of Technology, New Delhi, India.

Thanking you,

Organizing Committee  
ICAMET-2023  
Website: [www.icamet.in](http://www.icamet.in)

### APPENDIX 3 REGISTRATION SLIP FOR PROOF OF CONFERENCE REGISTRATION


**INTERNATIONAL CONFERENCE ON  
ADVANCED MATERIALS FOR EMERGING TECHNOLOGIES**  
 May 4-6, 2023  
 Department of Physics  
 Netaji Subhas University of Technology (NSUT)  
 Sec-3, Dwarka, New Delhi-110078, India

**RECEIPT**


No. **072** Date 04.05.2023

Received with thanks from Prof./Dr./Mr./Ms. Shubda Kaushik

a Sum of Rupees (in words) Two thousand only

on account of Registration/Accommodation/Miscellaneous .....

..... by online Transfer transaction ID No. UPI/348137- Dated 04.05.2023

₹ 2000/- 68 2667


### APPENDIX 4 CERTIFICATE OF CONFERENCE PAPER





**Department of Physics**  
 Netaji Subhas University of Technology  
 Sec-3, Dwarka, New Delhi-110078, India

**Certificate of Presentation**

This certificate is proudly awarded to Prof./Dr./Mr./Ms. Shubda Kaushik  
 from DTU, New Delhi

Paper Title: To study the impact of several ETLs - - - - - SCAPS-ID

For your excellent oral/ poster presentation at the conference and your significant contribution to the success of **International Conference on Advanced Materials for Emerging Technologies (ICAMET- 2023)**, held during **May 4-6, 2023**, at Netaji Subhas University of Technology, New Delhi - 110078, India.





Dr. Anurag Gaur  
 Convener Prof. Ranjana Jha  
 Conference Chair

## APPENDIX 5 PROOF OF SCOPUS INDEXING

Themes of Conference	Registration fee	Abstract submission
<ul style="list-style-type: none"> <li>❖ Functional Nanomaterials</li> <li>❖ Metals, Alloys, Ceramics and Polymer</li> <li>❖ Materials Synthesis &amp; Characterization</li> <li>❖ Optical/electronic/ magnetic materials</li> <li>❖ Energy Materials and Devices</li> <li>❖ Solar and Renewable Energy</li> <li>❖ Smart Materials and Systems</li> <li>❖ Carbon Based Materials</li> <li>❖ Hydrogen and Biomass Energy</li> <li>❖ Green Energy and Environment</li> <li>❖ Biomaterials and Tissue Engineering</li> <li>❖ Super-capacitors and Batteries</li> <li>❖ Water Remediation / Treatment</li> <li>❖ Materials for Emerging Technologies</li> </ul>	Students : INR ₹2000 Faculty/Scientist : INR ₹5000 Industry participants : INR ₹6000 Foreign Delegates : USD 200  Registration fee will include registration kit, lunch, dinner, tea/coffee during sessions.	The abstract (max. one page as per template) shall be submitted through website: <a href="http://www.icamet.in">www.icamet.in</a>  <b>Further details regarding abstract submission and registration are available on conference website <a href="http://www.icamet.in">www.icamet.in</a></b>  <b>e-mail: <a href="mailto:icamet@nsut.ac.in">icamet@nsut.ac.in</a></b>  The conference will be in hybrid (Online and Offline) mode. Abstract book will be published. The full length peer reviewed selected papers of ICAMET 2023 will be published in SCI/Scopus journal.
<b>Important dates</b> Abstract submission closes : 15 April 2023 Registration opens : 16 April 2023 Registration closes : 25 April 2023		
<b>Venue: APJ-11, NSUT Campus, Sector 3, Dwarka, New Delhi-110078</b>		
<b>There will be three cash awards for best oral and poster presentations in each category.</b>		
<b>Contacts: Convener Dr. Anurag Gaur 9896087178, Co-Convener Dr. Harsh Yadav 8802273723</b>		
<b>The tariffs for exhibition and souvenir advertisement are available on the conference website.</b>		
<b>Tourism in Delhi:</b> Delhi is famous for its heritage sites, featuring UNESCO Heritage sites like Red Fort, Akshardham Temple, Humayun's Tomb, Jama Masjid and Qutub Minar etc.		

## APPENDIX 6 PROOF OF SUBMISSION MAIL (PAPER 2)

The screenshot shows an email from Materials Science & Engineering B (em@editorialmanager.com) dated May 12, 2023, 9:31 PM. The subject is "MSB-D-23-00851 - Confirming your submission to Materials Science & Engineering B". The email content is as follows:

Dear Mr. DESWAL,

Thank you for sending your manuscript Numerical simulation of highly efficient Cs<sub>2</sub>AgnBr<sub>6</sub>-based Double Perovskite Solar Cell using SCAPS 1-D for consideration to Materials Science & Engineering B. Please accept this message as confirmation of your submission. It has been assigned the following manuscript number: MSB-D-23-00851.

**When should I expect to receive the Editor's decision?**  
 We publicly share the average editorial times for Materials Science & Engineering B to give you an indication of when you can expect to receive the Editor's decision. These can viewed here: [http://journalinsights.elsevier.com/journals/0921-5107/review\\_speed](http://journalinsights.elsevier.com/journals/0921-5107/review_speed)

**What happens next?**  
 Here are the steps that you can expect as your manuscript progresses through the editorial process in the Editorial Manager (EM).

1. First, your manuscript will be assigned to an Editor and you will be sent a unique reference number that you can use to track it throughout the process. During this stage, the status in EM will be "With Editor".
2. If your manuscript matches the scope and satisfies the criteria of Materials Science & Engineering B, the Editor will identify and contact reviewers who are acknowledged experts in the field. Since peer-review is a voluntary service, it can take some time but please be assured that the Editor will regularly remind reviewers; if they do not reply in a timely manner. During this stage, the status will appear as "Under Review".

Once the Editor has received the minimum number of expert reviews, the status will change to "Required Reviews Complete".

3. It is also possible that the Editor may decide that your manuscript does not meet the journal criteria or scope and that it should not be considered further. In this case, the Editor will immediately notify you that the manuscript has been rejected and may recommend a more suitable journal.

## APPENDIX 7 PROOF OF SCOPUS INDEXING OF JOURNAL

The screenshot displays the ScienceDirect website for the journal "Materials Science and Engineering: B". The page features a dark blue header with the journal title and a "Submit your article" button. Below the header, there are navigation links for "Articles & Issues", "About", "Publish", "Order journal", and a search bar. The main content area highlights a "Publishing timeline" of "1.6 weeks" and lists "Abstracting and indexing" services. The footer includes the Elsevier logo, a cookie notice, and a "FEEDBACK" button.

**Materials Science and Engineering: B** | Supports open access

Submit your article ↗

Articles & Issues ▾ About ▾ Publish ▾ Order journal ↗ 🔍 Search in this journal Guide for authors ↗

Publishing timeline

**1.6 weeks**  
Publication Time ⓘ

Abstracting and indexing

- Chemical Abstracts
- Science Citation Index
- American Ceramic Society
- Research Alert
- Cambridge Scientific Abstracts
- Current Contents
- Engineering Index
- Glass Technology Abstracts
- INSPEC
- Metals Abstracts
- Pascal Francis
- Physikalische Berichte
- Fluid Abstracts
- FLUIDEX
- RIZ Karlsruhe
- Scopus

[View historical data and other metrics >](#)

About ScienceDirect Remote access Shopping cart Advertise Contact and support Terms and conditions Privacy policy

**ELSEVIER** We use cookies to help provide and enhance our service and tailor content and ads. By continuing you agree to the use of cookies.  
Copyright © 2023 Elsevier B.V. or its licensors or contributors. ScienceDirect® is a registered trademark of Elsevier B.V.

**RELX™**

FEEDBACK ⓘ

30°C Haze Search ENG IN 22:36 28-05-2023

## References

- [1] D. B. Mitzi, "Templating and structural engineering in organic–inorganic perovskites," *Journal of the Chemical Society, Dalton Transactions*, no. 1, pp. 1–12, 2001, doi: 10.1039/b007070j.
- [2] M. Kibbou, Y. Benhouria, M. Boujnah, I. Essaoudi, A. Ainane, and R. Ahuja, "The electronic, magnetic and electrical properties of  $\text{Mn}_2\text{FeReO}_6$ : Ab-initio calculations and Monte-Carlo simulation," *J Magn Magn Mater*, vol. 495, p. 165833, Feb. 2020, doi: 10.1016/j.jmmm.2019.165833.
- [3] M. Kibbou *et al.*, " $\text{Cs}_2\text{InGaX}_6$  (X=Cl, Br, or I): Emergent Inorganic Halide Double Perovskites with enhanced optoelectronic characteristics," *Current Applied Physics*, vol. 21, pp. 50–57, Jan. 2021, doi: 10.1016/j.cap.2020.10.007.
- [4] M. Anaya, G. Lozano, M. E. Calvo, and H. Míguez, "ABX<sub>3</sub> Perovskites for Tandem Solar Cells," *Joule*, vol. 1, no. 4, pp. 769–793, Dec. 2017, doi: 10.1016/j.joule.2017.09.017.
- [5] C. Yi *et al.*, "Entropic stabilization of mixed A-cation ABX<sub>3</sub> metal halide perovskites for high performance perovskite solar cells," *Energy Environ Sci*, vol. 9, no. 2, pp. 656–662, 2016, doi: 10.1039/C5EE03255E.
- [6] C. C. Boyd, R. Cheacharoen, T. Leijtens, and M. D. McGehee, "Understanding Degradation Mechanisms and Improving Stability of Perovskite Photovoltaics," *Chem Rev*, vol. 119, no. 5, pp. 3418–3451, Mar. 2019, doi: 10.1021/acs.chemrev.8b00336.
- [7] A. Babayigit, A. Ethirajan, M. Muller, and B. Conings, "Toxicity of organometal halide perovskite solar cells," *Nat Mater*, vol. 15, no. 3, pp. 247–251, Mar. 2016, doi: 10.1038/nmat4572.
- [8] W. Ke and M. G. Kanatzidis, "Prospects for low-toxicity lead-free perovskite solar cells," *Nat Commun*, vol. 10, no. 1, p. 965, Feb. 2019, doi: 10.1038/s41467-019-08918-3.
- [9] J. C. Dahl *et al.*, "Probing the Stability and Band Gaps of  $\text{Cs}_2\text{AgInCl}_6$  and  $\text{Cs}_2\text{AgSbCl}_6$  Lead-Free Double Perovskite Nanocrystals," *Chemistry of Materials*, vol. 31, no. 9, pp. 3134–3143, May 2019, doi: 10.1021/acs.chemmater.8b04202.
- [10] C. Wu *et al.*, "The Dawn of Lead-Free Perovskite Solar Cell: Highly Stable Double Perovskite  $\text{Cs}_2\text{AgBiBr}_6$  Film," *Advanced Science*, vol. 5, no. 3, p. 1700759, Mar. 2018, doi: 10.1002/advs.201700759.

- [11] Z. Xiao, Z. Song, and Y. Yan, "From Lead Halide Perovskites to Lead-Free Metal Halide Perovskites and Perovskite Derivatives," *Advanced Materials*, vol. 31, no. 47, p. 1803792, Nov. 2019, doi: 10.1002/adma.201803792.
- [12] E. Meyer, D. Mutukwa, N. Zingwe, and R. Taziwa, "Lead-Free Halide Double Perovskites: A Review of the Structural, Optical, and Stability Properties as Well as Their Viability to Replace Lead Halide Perovskites," *Metals (Basel)*, vol. 8, no. 9, p. 667, Aug. 2018, doi: 10.3390/met8090667.
- [13] M. Kibbou, Z. Haman, N. Khossossi, I. Essaoudi, A. Ainane, and R. Ahuja, "Computational insights into the superior efficiency of Cs<sub>2</sub>AgGa(Cl,Br)<sub>6</sub> double halide perovskite solar cells," *Mater Chem Phys*, vol. 294, p. 126978, Jan. 2023, doi: 10.1016/j.matchemphys.2022.126978.
- [14] A. Walsh, "Principles of Chemical Bonding and Band Gap Engineering in Hybrid Organic–Inorganic Halide Perovskites," *The Journal of Physical Chemistry C*, vol. 119, no. 11, pp. 5755–5760, Mar. 2015, doi: 10.1021/jp512420b.
- [15] J. Yang, "Game-theoretic modeling of players' ambiguities on external factors," *J Math Econ*, vol. 75, pp. 31–56, 2018, doi: <https://doi.org/10.1016/j.jmateco.2017.12.008>.
- [16] R. Fu *et al.*, "Pressure-induced structural transition and band gap evolution of double perovskite Cs<sub>2</sub>AgBiBr<sub>6</sub> nanocrystals," *Nanoscale*, vol. 11, no. 36, pp. 17004–17009, 2019, doi: 10.1039/C9NR07030C.
- [17] G. García-Espejo, D. Rodríguez-Padrón, R. Luque, L. Camacho, and G. de Miguel, "Mechanochemical synthesis of three double perovskites: Cs<sub>2</sub>AgBiBr<sub>6</sub>, (CH<sub>3</sub>NH<sub>3</sub>)<sub>2</sub>TiBiBr<sub>6</sub> and Cs<sub>2</sub>AgSbBr<sub>6</sub>," *Nanoscale*, vol. 11, no. 35, pp. 16650–16657, 2019, doi: 10.1039/C9NR06092H.
- [18] Z. Zhang, Z. Wu, D. Rincon, C. Garcia, and P. D. Christofides, "Operational safety of chemical processes via Safeness-Index based MPC: Two large-scale case studies," *Comput Chem Eng*, vol. 125, pp. 204–215, 2019, doi: <https://doi.org/10.1016/j.compchemeng.2019.03.003>.
- [19] L. Schade *et al.*, "Structural and Optical Properties of Cs<sub>2</sub>AgBiBr<sub>6</sub> Double Perovskite," *ACS Energy Lett*, vol. 4, no. 1, pp. 299–305, Jan. 2019, doi: 10.1021/acsenergylett.8b02090.

- [20] N. M. Ravindra, P. Ganapathy, and J. Choi, "Energy gap–refractive index relations in semiconductors – An overview," *Infrared Phys Technol*, vol. 50, no. 1, pp. 21–29, 2007, doi: <https://doi.org/10.1016/j.infrared.2006.04.001>.
- [21] S. Adachi, "Band gaps and refractive indices of AlGaAsSb, GaInAsSb, and InPAsSb: Key properties for a variety of the 2-4- $\mu\text{m}$  optoelectronic device applications," *J Appl Phys*, vol. 61, no. 10, pp. 4869–4876, 1987, doi: [10.1063/1.338352](https://doi.org/10.1063/1.338352).
- [22] G. Volonakis *et al.*, "Cs<sub>2</sub>InAgCl<sub>6</sub>: A New Lead-Free Halide Double Perovskite with Direct Band Gap," *J Phys Chem Lett*, vol. 8, no. 4, pp. 772–778, Feb. 2017, doi: [10.1021/acs.jpcclett.6b02682](https://doi.org/10.1021/acs.jpcclett.6b02682).
- [23] Z. Zhang *et al.*, "Potential Applications of Halide Double Perovskite Cs<sub>2</sub>AgInX<sub>6</sub> (X = Cl, Br) in Flexible Optoelectronics: Unusual Effects of Uniaxial Strains," *J Phys Chem Lett*, vol. 10, no. 5, pp. 1120–1125, Mar. 2019, doi: [10.1021/acs.jpcclett.9b00134](https://doi.org/10.1021/acs.jpcclett.9b00134).
- [24] Y. Liang, "Exploring inorganic and nontoxic double perovskites Cs<sub>2</sub>AgInBr<sub>6</sub>(1-x)Cl<sub>6x</sub> from material selection to device design in material genome approach," *J Alloys Compd*, vol. 862, p. 158575, 2021, doi: <https://doi.org/10.1016/j.jallcom.2020.158575>.
- [25] M. K. Hossain, M. H. K. Rubel, G. F. I. Toki, I. Alam, M. F. Rahman, and H. Bencherif, "Effect of Various Electron and Hole Transport Layers on the Performance of CsPbI<sub>3</sub>-Based Perovskite Solar Cells: A Numerical Investigation in DFT, SCAPS-1D, and wxAMPS Frameworks," *ACS Omega*, vol. 7, no. 47, pp. 43210–43230, Nov. 2022, doi: [10.1021/acsomega.2c05912](https://doi.org/10.1021/acsomega.2c05912).
- [26] K. Deepthi Jayan and V. Sebastian, "Modelling and comparative performance analysis of tin based mixed halide perovskite solar cells with <sc>IGZO</sc> and <sc>CuO</sc> as charge transport layers," *Int J Energy Res*, vol. 45, no. 11, pp. 16618–16632, Sep. 2021, doi: [10.1002/er.6909](https://doi.org/10.1002/er.6909).
- [27] A. Hima, "Enhancing of CH<sub>3</sub>NH<sub>3</sub>SnI<sub>3</sub> based solar cell efficiency by ETL engineering," *International Journal of Energetica*, vol. 5, no. 1, p. 27, Jul. 2020, doi: [10.47238/ijeca.v5i1.119](https://doi.org/10.47238/ijeca.v5i1.119).
- [28] Y. Raoui, H. Ez-Zahraouy, N. Tahiri, O. El Bounagui, S. Ahmad, and S. Kazim, "Performance analysis of MAPbI<sub>3</sub> based perovskite solar cells employing diverse

charge selective contacts: Simulation study," *Solar Energy*, vol. 193, pp. 948–955, 2019, doi: <https://doi.org/10.1016/j.solener.2019.10.009>.

[29] S. Abdelaziz, A. Zekry, A. Shaker, and M. Abouelatta, "Investigating the performance of formamidinium tin-based perovskite solar cell by SCAPS device simulation," *Opt Mater (Amst)*, vol. 101, p. 109738, 2020, doi: <https://doi.org/10.1016/j.optmat.2020.109738>.

[30] N. K. Sinha, D. S. Ghosh, and A. Khare, "Role of built-in potential over ETL/perovskite interface on the performance of HTL-free perovskite solar cells," *Opt Mater (Amst)*, vol. 129, p. 112517, 2022, doi: <https://doi.org/10.1016/j.optmat.2022.112517>.

[31] I. Chabri, A. Oubelkacem, and Y. Benhouria, "Numerical development of lead-free  $\text{Cs}_2\text{Tl}_6$ -based perovskite solar cell via SCAPS-1D," in *E3S Web of Conferences*, B. Benhala, K. Mansouri, A. Raihani, and M. Qbadou, Eds., Jan. 2022, p. 00050. doi: [10.1051/e3sconf/202233600050](https://doi.org/10.1051/e3sconf/202233600050).

[32] S. Ahmmed, A. Aktar, J. Hossain, and A. B. Md. Ismail, "Enhancing the open circuit voltage of the SnS based heterojunction solar cell using NiO HTL," *Solar Energy*, vol. 207, pp. 693–702, Sep. 2020, doi: [10.1016/j.solener.2020.07.003](https://doi.org/10.1016/j.solener.2020.07.003).

[33] K. Sobayel *et al.*, "A comprehensive defect study of tungsten disulfide (WS<sub>2</sub>) as electron transport layer in perovskite solar cells by numerical simulation," *Results Phys*, vol. 12, pp. 1097–1103, Mar. 2019, doi: [10.1016/j.rinp.2018.12.049](https://doi.org/10.1016/j.rinp.2018.12.049).

[34] L. Huang *et al.*, "Electron transport layer-free planar perovskite solar cells: Further performance enhancement perspective from device simulation," *Solar Energy Materials and Solar Cells*, vol. 157, pp. 1038–1047, 2016, doi: <https://doi.org/10.1016/j.solmat.2016.08.025>.

[35] Most. M. Khatun, A. Sunny, and S. R. Al Ahmed, "Numerical investigation on performance improvement of WS<sub>2</sub> thin-film solar cell with copper iodide as hole transport layer," *Solar Energy*, vol. 224, pp. 956–965, Aug. 2021, doi: [10.1016/j.solener.2021.06.062](https://doi.org/10.1016/j.solener.2021.06.062).

[36] Yan Wang, Zhonggao Xia, Yiming Liu, and Hang Zhou, "Simulation of perovskite solar cells with inorganic hole transporting materials," in *2015 IEEE 42nd Photovoltaic Specialist Conference (PVSC)*, IEEE, Jun. 2015, pp. 1–4. doi: [10.1109/PVSC.2015.7355717](https://doi.org/10.1109/PVSC.2015.7355717).



- [37] N. Touafek, R. amdane Mahamdi, and C. Dridi, "Boosting the performance of planar inverted perovskite solar cells employing graphene oxide as HTL," *Digest Journal of Nanomaterials and Biostructures*, vol. 16, no. 2, pp. 705–712, 2021, [Online]. Available: [https://chalcogen.ro/705\\_TouafekN.pdf](https://chalcogen.ro/705_TouafekN.pdf)
- [38] H. Alipour and A. Ghadimi, "Optimization of lead-free perovskite solar cells in normal-structure with  $\text{WO}_3$  and water-free PEDOT: PSS composite for hole transport layer by SCAPS-1D simulation," *Opt Mater (Amst)*, vol. 120, p. 111432, Oct. 2021, doi: 10.1016/j.optmat.2021.111432.
- [39] Y. H. Khattak, F. Baig, H. Toura, S. Beg, and B. M. Soucase, "CZTSe Kesterite as an Alternative Hole Transport Layer for MASnI<sub>3</sub> Perovskite Solar Cells," *J Electron Mater*, vol. 48, no. 9, pp. 5723–5733, 2019, doi: 10.1007/s11664-019-07374-5.
- [40] M. Kibbou, Z. Haman, N. Khossossi, I. Essaoudi, A. Ainane, and R. Ahuja, "Computational insights into the superior efficiency of Cs<sub>2</sub>AgGa(Cl,Br)<sub>6</sub> double halide perovskite solar cells," *Mater Chem Phys*, vol. 294, p. 126978, Jan. 2023, doi: 10.1016/j.matchemphys.2022.126978.
- [41] K. Q. Wang, Y. He, M. Zhang, J. J. Shi, and W. W. Cai, "Promising Lead-Free Double-Perovskite Photovoltaic Materials Cs<sub>2</sub>MM'Br<sub>6</sub> (M = Cu, Ag, and Au; M' = Ga, In, Sb, and Bi) with an Ideal Band Gap and High Power Conversion Efficiency," *Journal of Physical Chemistry C*, vol. 125, no. 38, pp. 21160–21168, Sep. 2021, doi: 10.1021/acs.jpcc.1c05699.
- [42] A. Menedjhi, N. Bouarissa, S. Saib, and K. Bouamama, "Halide double perovskite Cs<sub>2</sub>AgInBr<sub>6</sub> for photovoltaic's applications: Optical properties and stability," *Optik (Stuttg)*, vol. 243, Oct. 2021, doi: 10.1016/j.ijleo.2021.167198.
- [43] M. Burgelman, K. Decock, S. Khelifi, and A. Abass, "Advanced electrical simulation of thin film solar cells," *Thin Solid Films*, vol. 535, pp. 296–301, 2013, doi: <https://doi.org/10.1016/j.tsf.2012.10.032>.
- [44] M. Burgelman, P. Nollet, and S. Degrave, "Modelling polycrystalline semiconductor solar cells," *Thin Solid Films*, vol. 361–362, pp. 527–532, 2000, doi: [https://doi.org/10.1016/S0040-6090\(99\)00825-1](https://doi.org/10.1016/S0040-6090(99)00825-1).
- [45] F. Liu *et al.*, "Numerical simulation: Toward the design of high-efficiency planar perovskite solar cells," *Appl Phys Lett*, vol. 104, no. 25, p. 253508, Jun. 2014, doi: 10.1063/1.4885367.

- [46] X. Meng *et al.*, "Optimization of germanium-based perovskite solar cells by SCAPS simulation," *Opt Mater (Amst)*, vol. 128, Jun. 2022, doi: 10.1016/j.optmat.2022.112427.
- [47] P. Sawicka-Chudy *et al.*, "Simulation of TiO<sub>2</sub>/CuO solar cells with SCAPS-1D software," *Mater Res Express*, vol. 6, no. 8, p. 085918, Jun. 2019, doi: 10.1088/2053-1591/ab22aa.
- [48] X. Li *et al.*, "Low-Temperature Solution-Processed ZnSe Electron Transport Layer for Efficient Planar Perovskite Solar Cells with Negligible Hysteresis and Improved Photostability," *ACS Nano*, vol. 12, no. 6, pp. 5605–5614, Jun. 2018, doi: 10.1021/acsnano.8b01351.